PERGAMON

Atmospheric Environment 36 (2002) 537–560

ATMOSPHERIC ENVIRONMENT

www.elsevier.com/locate/atmosenv

Modelling gaseous dry deposition in AURAMS: a unified regional air-quality modelling system

Leiming Zhang*, Michael D. Moran, Paul A. Makar, Jeffrey R. Brook, Sunling Gong

Meteorological Service of Canada, 4905 Dufferin Street, Toronto, Ont., Canada M3H 5T4

Received 5 May 2001; accepted 21 August 2001

Abstract

An upgraded parameterization scheme for gaseous dry-deposition velocities has been developed for a new regional air-quality model with a 91-species gas-phase chemistry mechanism, of which 48 species are "transported" species. The well-known resistance analogy to dry deposition is adopted in the present scheme, with both O_3 and SO_2 taken as base species. Stomatal resistances are calculated for all dry-depositing species using a "sunlit/shaded big-leaf" canopy stomatal resistance submodel. Dry-ground, wet-ground, dry-cuticle, and wet-cuticle resistances for O_3 and SO_2, and parameters for calculating canopy stomatal resistance and aerodynamic resistance for these two base species are given as input parameters for each of the 15 land-use categories and/or five seasonal categories considered by the scheme. Dry-ground, wet-ground, dry-cuticle, and wet-cuticle resistances for the other 29 model species for which dry deposition is considered to be a significant process are scaled to the resistances of O_3 and SO_2 based on published measurements of their dry deposition and/or their aqueous solubility and oxidizing capacity. Mesophyll resistances are treated as dependent only on chemical species. Field experimental data have then been used to evaluate the scheme's performance for O_3 and SO_2. Example sets of modelled dry-deposition velocities have also been calculated for all 31 dry-deposited species and 15 land-use categories for different environmental conditions. This new scheme incorporates updated information on dry-deposition measurements and is able to predict deposition velocities for 31 gaseous species for different land-use types, seasons, and meteorological conditions.

Keywords: Air-quality modelling; Gaseous species; Dry deposition; Deposition velocity; Big-leaf model; Surface resistance

1. Introduction

A new regional particulate-matter (PM) air-quality model is being developed by the Meteorological Service of Canada (MSC). The acronym for this new model is AURAMS, which stands for "A Unified Regional Air-quality Modelling System" (Moran et al., 1998). AURAMS is intended to provide a better understanding of PM and other regional pollutants in North America, and especially in Canada. The model will be capable of assessing the impact of emission reduction scenarios separately or simultaneously for PM, ground-level ozone, acidic deposition, and, eventually, air toxics. To take as much advantage as possible of the work in regional air quality modelling already carried out at MSC (formerly the Atmospheric Environment Service), AURAMS makes use of four existing MSC air-quality-related models or modules as "building blocks". These existing models include (i) the Chemical Tracer Model/Mesoscale Compressible Community Model (CTM/MC2), a regional-scale photochemical oxidant model coupled with a prognostic meteorological model

*Corresponding author. Tel.: +1-416-739-5734; fax: +1-416-739-5704.

E-mail address: leiming.zhang@ec.gc.ca (L. Zhang).

1352-2310/02/$ - see front matter
PII: S1352-2310(01)00447-2

(Pudykiewicz et al., 1997), (ii) the Acid Deposition and Oxidant Model (ADOM), a comprehensive, episodic regional acid deposition model (Venkatram et al., 1988), and (iii) the Canadian Aerosol Module (CAM), a composition- and size-resolved aerosol module that has already been used within both a global and a regional climate model (Gong et al., 2001). The fourth building block is the Canadian Emissions Processing System (CEPS), an emissions modelling system for regional-scale air quality models that is needed to create emissions input files (Moran et al., 1997).

Dry deposition is an important process that requires treatment in AURAMS. A size-segregated particle dry deposition module originally developed for CAM (Zhang et al., 2001b) has been incorporated into AURAMS to treat particle dry deposition. For representing gaseous dry deposition, however, the existing MSC modules are less attractive and many aspects need to be modified and updated to reflect more recent advances. Some newer dry-deposition schemes include treatments of vertical canopy structure (e.g., Baldocchi and Meyers, 1998; Meyers et al., 1998), NH_3 compensation points (Sutton et al., 1998; Flechard et al., 1999), in-canopy radiation processes and air–soil interactions (Sellers et al., 1996), and chemical equilibrium (Padro et al., 1998), but these schemes are either computationally demanding or require detailed biological, physical and/or chemical knowledge. Instead, a simpler approach known as big-leaf models (e.g., Pleim et al., 1984; Wesely, 1989; Erisman et al., 1994b; Smith et al., 2000) has been adopted for AURAMS. One reason for this choice in the context of regional air-quality modelling is the need to balance the accuracy, complexity, and computational cost of the parameterization for dry deposition with the parameterizations of the many other processes that must be represented. A second reason for choosing a relatively simple dry-deposition scheme is that such schemes are likely to produce deposition estimates that are as reliable or representative as results from more sophisticated schemes. This is because dry deposition is very sensitive to surface conditions and our knowledge of dry-deposition processes is still limited.

Existing big-leaf models cannot be adopted directly, however, due to the fact that the AURAMS gas-phase chemical mechanism has many additional chemical species for which dry deposition must also be addressed. Besides those gaseous species that are usually considered by the dry-deposition community (i.e., SO_2, O_3, HNO_3, NO_2), there are more than 40 other AURAMS species that are long-lived enough for transport to be considered and whose dry deposition may also need to be represented. The land-use categorization used by AURAMS is also different from the categorizations employed in the above-mentioned schemes, and thus some adaptation is required. In the present study, we use the big-leaf-model approach but also extend the treatment of dry deposition to the other chemical species required by AURAMS based on two master species, O_3 and SO_2, and try to incorporate the latest measurement data on dry deposition. The same land-use categories (LUCs) and seasonal categories (SCs) as used in the CAM dry-deposition model for particles (Zhang et al., 2001b) are also used here for gaseous species. Note that biogenic emissions, the role of compensation points, rapid chemical reactions in the air near the surface, and species lipid solubility are not considered in the dry-deposition model explicitly, though two of these (biogenic emissions, gas-phase chemical reactions) are considered in other parts of AURAMS.

The next section describes in more detail the formulation of the various resistance components for each land-use and seasonal category. Topics covered include the identification of the AURAMS gas-phase chemical species for which dry deposition is judged to be a significant process and the choice of scaling parameters for the resistances of other species relative to O_3 and SO_2 resistances. Performance-evaluation and model example results are then presented in Section 3, and Section 4 closes the paper with a summary of findings.

2. Formulation of resistance components

Using the well-known resistance analogy to dry deposition, the dry-deposition velocity V_d is defined to be the inverse of total resistance R_t. R_t consists of the sum of aerodynamic resistance, R_a, quasi-laminar sublayer resistance, R_b, and surface or canopy resistance, R_c (e.g., Wesely and Hicks, 2000). R_a is only a function of micrometeorological conditions and the roughness characteristics of the underlying surface, so it is independent of chemical species. Since the top of the first model layer for AURAMS is located at 15 m, a height usually within the surface layer, the aerodynamic resistance is calculated using a simple formula from Padro (1996). R_b is a function of friction velocity and the molecular diffusivity of each chemical species. The simple approach as used in Padro (1996) is adopted here to determine R_b, although more sophisticated treatments for R_b are also available for some species (e.g., Massman, 1999).

The surface resistance R_c is the most important and complex resistance for most gaseous species and effectively determines whether a species is dry deposited or not. R_c is parameterized here as a set of parallel resistances:

$$\frac{1}{R_c} = \frac{1 - W_{st}}{R_{st} + R_m} + \frac{1 - W_c}{R_{cutd}} + \frac{W_c}{R_{cutw}} + \frac{1 - W_g}{R_{gd}} + \frac{W_g}{R_{gw}}, \quad (1)$$

where W_{st} is the fraction of stomatal closure when the leaves are wet, W_c is the fraction of canopy that is wet (if there is a canopy), W_g is the fraction of the ground surface that is wet, and R_{st}, R_m, R_{cutd}, R_{cutw}, R_{gd}, and R_{gw} are the canopy stomatal, mesophyll, dry-cuticle, wet-cuticle, dry-ground, and wet-ground resistances, respectively. For unvegetated surfaces, only W_g, R_{gd}, and R_{gw} need to be considered. The in-canopy aerodynamic resistance (Erisman et al., 1994b; Wesely, 1989) is not explicitly considered in Eq. (1) but is included implicitly in the values of R_{gd} and R_{gw}. Details of the representations of each of the nine variables in Eq. (1) are discussed in the following sections.

2.1. W_c, W_g, and W_{st}

For rainy, dewy, or highly humid conditions, the canopy and ground may be fully or partially wet. During rainy conditions, the canopy and ground are usually fully wet, but the undersides of leaves may still be dry. Under dewy conditions, especially for high canopies, the canopy leaves should be mostly wet but the ground could be partially dry. For highly humid conditions (i.e., RH > 80%) without rain or dew, the canopy and ground may both be partially wet. Sellers et al. (1996) have suggested one method for calculating W_c and W_g. This method, however, requires detailed information about canopy and ground characteristics that is not available to the current model. In the present study, W_c is assigned values of 0.9, 0.7, and 0.2 and W_g is assigned values of 0.9, 0.5, and 0.2 for rainy, dewy, and humid conditions, respectively. Zhang et al. (2001a) suggested that stomata may not be completely covered even during rainy or dewy conditions. A value of 0.5 was used for W_{st} in Zhang et al. (2001a) under rainy or dewy conditions, and the same value is used here.

2.2. R_{st}

In the "sunlit/shaded big-leaf" canopy stomatal resistance model, which was referred to as the "two-big-leaf" model in Zhang et al. (2001c), the whole canopy is subdivided into sunlit leaves and shaded leaves. This model is adopted here for calculating canopy stomatal resistance R_{st}:

$$R_{st} = 1/[G_{st}(\mathrm{PAR}) f(T) f(D) f(\psi) D_i/D_v], \quad (2)$$

where $G_{st}(\mathrm{PAR})$ is the unstressed canopy stomatal conductance, a function of photosynthetically active radiation (PAR). The dimensionless functions $f(T)$, $f(D)$, and $f(\psi)$ represent the conductance-reducing effects of air temperature T, water vapour pressure deficit D, and water stress (leaf water potential) ψ, respectively, on leaf stomatal conductance. D_v and D_i are the molecular diffusivities for water vapour and the pollutant gas, respectively. Since leaf stomatal conductance varies with PAR, G_{st} is calculated as the weighted sum of conductances for sunlit and shaded leaves:

$$G_{st}(\mathrm{PAR}) = F_{sun}/r_{st}(\mathrm{PAR}_{sun}) + F_{shade}/r_{st}(\mathrm{PAR}_{shade}), \quad (3)$$

$$r_{st}(\mathrm{PAR}) = r_{st\,min}(1 + b_{rs}/\mathrm{PAR}), \quad (4)$$

where F_{sun} and F_{shade} are the total sunlit and shaded leaf area indexes (LAIs), respectively, PAR_{sun} and PAR_{shade} are PAR received by sunlit and shaded leaves, respectively, r_{st} is the unstressed leaf stomatal resistance, r_{stmin} is the minimum leaf stomatal resistance, and b_{rs} is an empirical constant.

The expressions for F_{sun} and F_{shade} are taken from Norman (1982):

$$F_{sun} = 2\cos\theta[1 - e^{(-0.5\mathrm{LAI}/\cos\theta)}], \quad (5)$$

$$F_{shade} = \mathrm{LAI} - F_{sun}. \quad (6)$$

The expressions for PAR_{sun} and PAR_{shade} are modified from Norman (1982) as discussed in Zhang et al. (2001c). For LAI < 2.5 or solar radiation $< 200\ \mathrm{W\,m^{-2}}$:

$$\mathrm{PAR}_{shade} = R_{diff} e^{(-0.5\mathrm{LAI}^{0.7})} + 0.07 R_{dir} \times (1.1 - 0.1\mathrm{LAI}) e^{-\cos\theta}, \quad (7)$$

$$\mathrm{PAR}_{sun} = R_{dir}\cos\alpha/\cos\theta + \mathrm{PAR}_{shade}. \quad (8)$$

For all other conditions:

$$\mathrm{PAR}_{shade} = R_{diff} e^{(-0.5\mathrm{LAI}^{0.8})} + 0.07 R_{dir} \times (1.1 - 0.1\mathrm{LAI}) e^{-\cos\theta}, \quad (9)$$

$$\mathrm{PAR}_{sun} = R_{dir}^{0.8}\cos\alpha/\cos\theta + \mathrm{PAR}_{shade}, \quad (10)$$

where LAI is the leaf area index of the canopy, θ is the solar zenith angle, and α is the angle between the leaf and the sun and has a value of 60° for a canopy assumed to have a spherical leaf angle distribution. R_{diff} and R_{dir} are the downward visible radiation fluxes above the canopy from diffuse and direct-beam radiation, respectively. Weiss and Norman (1985) developed formulas for calculating R_{diff} and R_{dir} from measured global incoming solar radiation, and these formulas are also used here.

The dimensionless functions $f(T)$, $f(D)$, and $f(\psi)$ are the same as used in Brook et al. (1999). Values for all parameters required for calculating R_{st} are taken from Brook et al. (1999), Dorman and Sellers (1989), and Dickinson et al. (1986). Zhang et al. (2001c) demonstrated that this two-big-leaf approach gives reasonable

estimates of canopy stomatal resistance for different vegetation types and LAI values.

2.3. R_m

Mesophyll resistance R_m is treated as dependent only on chemical species. For species with some degree of solubility and/or oxidizing capacity, R_m is negligible. Given the limited knowledge of R_m today, R_m is taken here to be $100\,s\,m^{-1}$ for species with both relatively limited solubility and very small oxidizing capacity and 0 for all of the other species. These values are within a reasonable range as estimated by the formula as a function of H^* given in Wesely (1989). The reason for not using a formula to estimate R_m in the present study is that the effective Henry's Law constant (H^*) has a range of values for some chemical species and is not known exactly for some other species (see Table 1). Values of R_m for all dry-depositing species in the new AURAMS gas-phase chemical mechanism are listed in Table 1.

2.4. R_{cutd}, R_{cutw}, R_{gd}, *and* R_{gw}

2.4.1. O_3 *and* SO_2

Similar to Brook et al. (1999) and Wesely (1989), dry-cuticle (R_{cutd}) and dry-ground (R_{gd}) resistances are treated as LUC- and SC-dependent. The 15 LUCs and 5 growing-season categories considered by Zhang et al. (2001b) are used here. Values of R_{cutd} and R_{gd} for O_3 and SO_2 by LUC and SC are listed in Table 2. When specifying dry-cuticle resistances, we assumed that canopies with larger LAIs and younger leaves have smaller cuticle resistances. When specifying soil resistances, we assumed that taller canopies have relatively larger ground resistances. This is based on the assumption that taller canopies have larger in-canopy aerodynamic resistances (Wesely, 1989; Erisman et al., 1994b), which is not explicitly treated in Eq. (1) but which is assumed to be included implicitly in the ground resistance terms. Canopies with constant wet soil have smaller ground resistances for SO_2 and slightly larger resistances for O_3. Observed dry-deposition velocities

Table 1
Chemical and physical parameters dependent upon chemical species[a]

No.	Symbol	Name	Depn Mmts	MW	H (M atm^{-1})	H^* (M atm^{-1})	pe^0 (W)	R_m	α	β
1	SO_2	Sulphur dioxide	Yes	64	$(1.1-1.5)\times10^0$	2.65×10^5	75.5 to −7.6	0	1	0
2	H_2SO_4	Sulphuric acid	No	98	2.1×10^5	$>2.1\times10^5$	4.9 to −4.3	0	1	1
—	NO	Nitric oxide	Yes	30	$(1.4–1.9)\times10^{-3}$	H	27.8–3.0	Not considered		
3	NO_2	Nitrogen dioxide	Yes	46	$(0.7–4.1)\times10^{-2}$	H	28.4–8.2	0	0	0.8
4	O_3	Ozone	Yes	48	$(0.9–1.3)\times10^{-2}$	H	28.1–18.6	0	0	1
5	H_2O_2	Hydrogen peroxide	Yes	34	$(0.7–1.4)\times10^5$	H	24.8–9.7	0	1	1
6	HNO_3	Nitric acid	Yes	63	$(0.1–2.6)\times10^6$	3.2×10^{13}	14.1–8.9	0	10	10
7	HONO	Nitrous acid	Yes	47	$(3.7–5.0)\times10^1$	2.6×10^5	17.5–14.8	0	2	2
8	HNO_4	Pernitric acid	No	79	$(0.1–1)\times10^5$	$>1\times10^7$	No data	0	5	5
9	NH_3	Ammonia	Yes	17	$(1.0–7.8)\times10^1$	1.1×10^4	Not applicable	0	1	0
10	PAN	Peroxyacetylnitrate	Yes	121	$(2.8–5.0)\times10^0$	H	30.2 to −1.5	0	0	0.6
11	PPN	Peroxypropylnitrate	No	135	2.9×10^0	H	37.8 to −2.3	0	0	0.6
12	APAN	Aromatic acylnitrate	No	183	No data	5	46.9–11.2	0	0	0.8
13	MPAN	Peroxymethacrylic nitric anhydride	No	147	1.7×10^0	H	3.1	0	0	0.3
14	HCHO	Formaldehyde	Yes	30	$(0.3–1.4)\times10^4$	4.9×10^3	3.0 to −0.1	0	0.8	0.2
15	MCHO	Acetaldehyde	No	44	$(1.0–1.7)\times10^1$	$\geqslant15$	−1.0 to −3.9	100	0	0.05
16	PALD	C3 carbonyls	No	58	$(2.4–3.7)\times10^0$	H	−1.3 to −1.8	100	0	0.05
17	C4A	C4–C5 carbonyls	No	72	$(0.9–1.8)\times10^1$	H	−1.3 to −1.8	100	0	0.05
18	C7A	C6–C8 carbonyls	No	128	$(0.4–11)\times10^1$	H	−1.5	100	0	0.05
19	ACHO	Aromatic carbonyls	No	106	$(3.5–4.2)\times10^1$	H	−1.0 to −2.5	100	0	0.05
20	MVK	Methyl-vinyl-ketone	No	70	$(2.1–4.4)\times10^1$	H	0.2	0	0	0.05
21	MACR	Methacrolein	No	70	$(4.3–6.5)\times10^0$	H	−1.2	100	0	0.05
22	MGLY	Methylgloxal	No	72	$(0.4–3.2)\times10^4$	H	−0.7	0	0.01	0
23	MOH	Methyl alcohol	No	32	$(1.4–2.3)\times10^2$	$\geqslant H$	3.0	0	0.6	0.1
24	ETOH	Ethyl alcohol	No	46	$(1.2–2.3)\times10^2$	$\geqslant H$	−1.3 to −2.9	0	0.6	0
25	POH	C3 alcohol	No	60	$(0.9–1.7)\times10^2$	$\geqslant H$	−0.3	0	0.4	0
26	CRES	Cresol	No	104	8.3×10^2	H	−2.5	0	0.01	0
27	FORM	Formic acid	Yes	46	$(0.9–8.9)\times10^3$	9.8×10^6	1.9 to −6.4	0	2	0
28	ACAC	Acetic acid	Yes	60	$(0.8–9.3)\times10^3$	9.6×10^5	−3.1 to −9.6	0	1.5	0
29	ROOH	Organic peroxides	Yes	48	$(0.1–3.1)\times10^2$	H	4.2–3.6	0	0.1	0.8
30	ONIT	Organic nitrates	No	77	2.0×10^0	H	10.5 to −5.0	100	0	0.5
31	INIT	Isoprene nitrate	No	147	2.0×10^0	H	No data	100	0	0.5

[a] Values for Henry's Law constant (H) were obtained from Howard and Meylan (1997) and Sander (1999). Effective Henry's Law constant (H^*) values were drawn from Table 5. pe^0(W) values were obtained from Table 6.

Table 2
Time-varying parameters used for modelling SO_2 and O_3 dry deposition velocities in AURAMS by land-use category[a] for five seasonal categories. For water surfaces, aerodynamic surface roughness z_0 is dependent on surface wind speed u (Na = not applicable)

	LUC													
Parameter	1	2	3	4	5	6	7	8	9	10	11	12	13/14	15
Seasonal category 1: Midsummer with lush vegetation														
LAI	5.2	4.5	1.1	3.4	4.5	2.0	2.0	0	0	0.5	0.2	0	0	0.3
z_0 (m)	0.8	2.65	0.85	1.05	1.15	0.1	0.1	0.04	0.03	0.1	0.03	0.01	z_0 (u)	1.0
R_{cutd} (SO_2) ($s\,m^{-1}$)	1000	1000	2000	1200	1000	1500	1500	Na	Na	4000	6000	Na	Na	6000
R_{cutd} (O_3) ($s\,m^{-1}$)	1000	1000	2000	1200	1000	1500	1500	Na	Na	4000	6000	Na	Na	6000
R_{gd} (SO_2) ($s\,m^{-1}$)	400	300	400	400	400	350	350	700	400	400	50	100	10	500
R_{gd} (O_3) ($s\,m^{-1}$)	500	600	450	500	500	400	400	500	800	400	1000	2000	2000	500
Seasonal category 2: Autumn with cropland before harvest														
LAI	5.2	4.5	0.8	1.9	3.5	1.5	1.5	0	0	2.5	0.2	0	0	0.2
z_0 (m)	0.9	2.65	0.9	1.05	1.15	0.1	0.1	0.04	0.03	0.1	0.03	0.01	z_0 (u)	1.0
R_{cutd} (SO_2) ($s\,m^{-1}$)	1500	1500	3000	2000	1500	2000	2000	Na	Na	1500	6000	Na	Na	6000
R_{cutd} (O_3) ($s\,m^{-1}$)	1500	1500	3000	2000	1500	2000	2000	Na	Na	1500	6000	Na	Na	6000
R_{gd} (SO_2) ($s\,m^{-1}$)	400	300	400	400	400	350	350	700	400	400	50	100	10	500
R_{gd} (O_3) ($s\,m^{-1}$)	500	600	450	500	500	400	400	500	800	400	1000	2000	2000	500
Seasonal category 3: Late autumn after harvest, no snow														
LAI	4.7	4.5	0.3	0.1	2.3	1.0	1.0	0	0	1.5	0.1	0	0	0.1
z_0 (m)	0.9	2.65	0.8	0.95	1.15	0.05	0.02	0.04	0.03	0.1	0.02	0.01	z_0 (u)	1.0
R_{cutd} (SO_2) ($s\,m^{-1}$)	2000	2000	8000	9000	2000	3000	3000	Na	Na	2000	9000	Na	Na	9000
R_{cutd} (O_3) ($s\,m^{-1}$)	2000	2000	8000	9000	2000	3000	3000	Na	Na	2000	9000	Na	Na	9000
R_{gd} (SO_2) ($s\,m^{-1}$)	400	300	400	400	400	350	350	700	400	400	50	100	10	500
R_{gd} (O_3) ($s\,m^{-1}$)	500	600	450	500	500	400	400	500	800	400	1000	2000	2000	500
Seasonal category 4: Winter, with or without snow, subfreezing														
LAI	5.5	4.5	0.0	0.0	2.3	0.5	0	0	0	1.2	0	0	0	0
z_0 (m)	0.9	2.65	0.55	0.55	1.15	0.02	0.02	0.04	0.03	0.10	0.02	0.01	z_0 (u)	1.0
R_{cutd} (SO_2) ($s\,m^{-1}$)	2000	2000	Na	Na	2000	6000	Na	Na	Na	3000	Na	Na	Na	Na
R_{cutd} (O_3) ($s\,m^{-1}$)	2000	2000	Na	Na	2000	6000	Na	Na	Na	3000	Na	Na	Na	Na
R_{gd} (SO_2) no snow	400	300	350	350	400	300	300	700	200	300	100	200	10	350
R_{gd} (O_3) no snow	700	600	700	700	700	700	700	700	1000	700	1000	2000	2000	1000
R_{gd} (SO_2) with snow	200	200	200	200	200	200	200	200	200	200	200	200	10	400
R_{gd} (O_3) with snow	3000	3000	3000	3000	3000	3000	3000	3000	3000	3000	3000	2000	2000	2000
Seasonal category 5: Transitional spring with partially green short annuals														
LAI	5.3	4.5	0.4	0.8	3.3	1.0	1.0	0	0	0.5	0.1	0	0	0.2
z_0 (m)	0.9	2.65	0.60	0.75	1.15	0.05	0.05	0.04	0.03	0.1	0.03	0.01	z_0 (u)	1.0
R_{cutd} (SO_2) ($s\,m^{-1}$)	1000	1000	4000	2000	1000	1500	1500	Na	Na	4000	6000	Na	Na	6000
R_{cutd} (O_3) ($s\,m^{-1}$)	1000	1000	4000	2000	1000	1500	1500	Na	Na	4000	6000	Na	Na	6000
R_{gd} (SO_2) ($s\,m^{-1}$)	400	300	400	400	400	350	350	700	400	400	50	100	10	500
R_{gd} (O_3) ($s\,m^{-1}$)	500	600	450	500	500	400	400	500	800	400	1000	2000	2000	500

[a] AURAMS land-use categories: (1) evergreen-needleleaf trees; (2) evergreen broadleaf trees; (3) deciduous needleleaf trees; (4) deciduous broadleaf trees; (5) mixed broadleaf and needleleaf trees; (6) grass; (7) crops, mixed farming; (8) desert; (9) tundra; (10) shrubs and interrupted woodlands; (11) wetlands with plants; (12) ice caps and glaciers; (13) inland water; (14) ocean; (15) urban.

during nighttime under dry conditions are also considered when specifying dry-cuticle and dry-ground resistances. For ground resistance during seasonal category 4 (winter season), we have separated it into two sub-categories: "with snow" and "without snow". For snow-covered surfaces, ground resistance is taken as $200\,s\,m^{-1}$ for SO_2 and $3000\,s\,m^{-1}$ for O_3 based on published V_d values over snow surfaces (e.g., Wesely et al., 1981). For surfaces without snow, SO_2 and O_3 resistances are considered for frozen or close to frozen conditions.

The effects of vegetative surface wetness on the removal of O_3 ranges from mildly inhibiting to significantly enhancing. For SO_2, surface wetness usually increases uptake substantially. Zhang et al. (2001a) have discussed wet-cuticle and wet-ground resistance of SO_2 and O_3. Due to our limited knowledge at present, wet-soil resistance for SO_2 is treated as independent of LUC and SC and is given a value of $100\,s\,m^{-1}$ for rainy and high-humidity conditions and $200\,s\,m^{-1}$ for dewy conditions. For O_3, wet-soil resistance is taken to be the same as dry-soil resistance. Wet-cuticle resistances for SO_2 and O_3 are parameterized as

$$R_{cw} = R_{cw0}(LAI + 0.1)^{-1/3}, \tag{11}$$

where R_{cw0} is an empirical constant and is taken to be $100\,s\,m^{-1}$ for SO_2 under rainy and high-humidity conditions, $200\,s\,m^{-1}$ for SO_2 under dewy conditions, $400\,s\,m^{-1}$ for O_3 under rainy and high-humidity conditions, and $800\,s\,m^{-1}$ for O_3 under dewy conditions. The constant 0.1 in Eq. (11) accounts for leafless canopies, since wet bark may also increase the uptake. Eq. (11) is based on the data presented in Finkelstein et al. (2000), studies reviewed in Zhang et al. (2001a), and some of our available data. Erisman et al. (1994b) developed a parameterization for R_{cw} for SO_2, and a constant of $1000\,s\,m^{-1}$ was chosen for O_3. Our study showed that, even for O_3, R_{cw} changed with wetness type (dew, rain, and high humidity). Further research is needed on this issue.

2.4.2. Other species

The contrasting chemical properties of O_3 and SO_2 provide a means of estimating the surface resistances of other substances by scaling according to measures of aqueous solubility and oxidizing capacity (Wesely, 1989; Wesely and Hicks, 2000). AURAMS has 48 transported species of which 31 are considered to dry deposit as described in this section. In the present scheme, similar to Wesely (1989), both SO_2 and O_3 are taken as base species. Dry-cuticle, wet-cuticle, dry-ground, and wet-ground resistances for all other species are then scaled to the resistances of SO_2 and O_3 as follows:

$$\frac{1}{R_{cutd}(i)} = \frac{\alpha(i)}{R_{cutd}(SO_2)} + \frac{\beta(i)}{R_{cutd}(O_3)}, \tag{12}$$

$$\frac{1}{R_{cutw}(i)} = \frac{\alpha(i)}{R_{cutw}(SO_2)} + \frac{\beta(i)}{R_{cutw}(O_3)}, \tag{13}$$

$$\frac{1}{R_{gd}(i)} = \frac{\alpha(i)}{R_{gd}(SO_2)} + \frac{\beta(i)}{R_{gd}(O_3)}, \tag{14}$$

$$\frac{1}{R_{gw}(i)} = \frac{\alpha(i)}{R_{gw}(SO_2)} + \frac{\beta(i)}{R_{gw}(O_3)}. \tag{15}$$

The array dimension i denotes chemical species. The values for parameters α and β must be chosen for each dry-depositing chemical species individually, and the basis for this choice is discussed next.

Published measurements of dry deposition are used as the primary basis for scaling. However, while there is enough information for some species (e.g., NO_2, HNO_3), there is only very limited or no information for some other species (e.g., organic nitrates). Thus, physical and chemical considerations based on aqueous solubility and aqueous oxidizing capacity are also used for scaling. Effective Henry's Law constants (H^*), which combine vapor pressure, solubility, and dissociation in water (e.g., Seinfeld and Pandis, 1998), can serve as a measure of aqueous solubility. Similar to Wesely (1989), values for the negative log of electron activity for half-redox reactions in neutral aqueous solutions $pe^0(W)$ are used to assess aqueous oxidizing capacity. The use of $pe^0(W)$ values as a reactivity surrogate must be approached with caution, however, since it is possible to generate a large range of half-redox reactions for the species of interest, and these values do not always correspond well to the observed V_d of the species involved (e.g., NO). Details on the methods for determining the H^* and $pe^0(W)$ values are presented in Appendices A and B (Tables 5 and 6) respectively.

Observations of V_d have been used to determine α and β whenever possible, and the α and β values that are based on H^* and $pe^0(W)$ values alone do not have the same degree of confidence as those based on ambient measurements. Nonetheless, H^* and $pe^0(W)$ values are a useful, though by no means complete, means of ranking species for which no measurements of V_d are available. In the absence of dry-deposition measurements, cuticle and ground resistances for species having larger $pe^0(W)$ values are scaled to those for O_3 based on best scientific judgement. For species with large H^* values, their cuticle and ground resistances are scaled to those for SO_2, again based on best scientific judgement. For species with both small $pe^0(W)$ (<-2.0) and H^* (<100) values, dry deposition is assumed to be negligible. On this basis, 31 out of the 48 AURAMS transported species are then judged to dry deposit. Physical Henry's Law constants (H), H^* values, and $pe^0(W)$ values, dry-deposition measurement data availability, and α and β values are listed in Table 1 for these 31 AURAMS dry deposited species (NO is also listed in Table 1, although its dry

deposition is not considered in the current study due to other reasons, i.e., soil emissions).

Since SO_2 and O_3 are the two base species used in the current dry-deposition scheme, α is set to 1 and β is set to 0 for SO_2 and α is set to 0 and β is set to 1 for O_3. α and β were then specified for the other dry-depositing species based on the following considerations (note that each individual or lumped species is initially referred to by its AURAMS symbol from Table 1).

H_2SO_4 (sulphuric acid vapour): Although no direct measurements of H_2SO_4 dry deposition have been made, the very high solubility and large oxidizing capacity of this species suggest that it will be deposited to all surfaces quite rapidly. The two scaling parameters α and β are both chosen as 1 for this species.

NO_2 (nitrogen dioxide): The limited solubility and fairly large oxidizing capacity of NO_2 might suggest a dry-deposition rate similar to O_3. However, this is probably true only when the ambient NO_2 concentration is not too small, conditions under which NO_x emissions and chemical reactions should not affect NO_2 deposition too much. There are a large number of measurements available for NO_2 dry deposition. Published measurements suggest that NO_2 has a much higher V_d during daytime than during nighttime over vegetated surfaces (Rondón et al., 1993; Walton et al., 1997), indicating the importance of stomatal uptake. The same reason applies for the higher NO_2 V_d observed over vegetated surfaces than over bare soil (Gravenhorst and Bottger, 1982). The low V_d values observed over water surfaces are consistent with its relatively limited solubility (Bottger et al., 1980). There are some field experiments for both NO_2 and O_3 conducted during the same time period at the same site. For example, Walton et al. (1997) found that daily maximum NO_2 V_d values could be the same as O_3 V_d values over a fruit orchard. This can be explained by stomatal uptake since stomatal resistance for O_3 and NO_2 are not expected to be much different. Rondón et al. (1993) found NO_2 V_d values to be smaller typically than O_3 V_d values for two pine forests and a spruce forest. Daytime NO_2 V_d values were 20–70% of O_3 V_d values and nighttime NO_2 V_d values were 30–100% of O_3 V_d values per projected needle area. Pilegaard et al. (1998) found the maximum daily dry-deposition velocity over harvested wheat to be $0.35\,cm\,s^{-1}$ while O_3 at the same site was $0.5\,cm\,s^{-1}$.

These smaller V_d values of NO_2 compared to O_3 may be caused in part by NO and/or NO_2 emissions (Hill, 1971). Wetness associated with dew or rain can either enhance or decrease NO_2 dry deposition (Eugster and Hesterberg, 1996), similar to the effect of wetness on O_3. Thus, we concluded that NO_2 and O_3 have similar behaviors for a variety of conditions (e.g., dry or wet, day or night) and land types, and NO_2 V_d is usually smaller than that of O_3. Parameters α and β are chosen here to be 0.0 and 0.8, respectively, which will give a V_d for NO_2 similar to that for O_3, but around 10–20% smaller.

NO (nitric oxide): Table 1 suggests that NO, like NO_2, has limited solubility and moderate oxidizing capacity. The aqueous reactivity given here is different from Wesely (1989), who ascribed a very low reactivity to NO and as a result assumed dry deposition of NO to be negligible. However, NO emissions from soils and chemical reactions are also known to affect NO deposition significantly (e.g., Padro et al., 1998). Given the ubiquity of NO soil emissions (e.g., Yienger and Levy, 1995), NO dry deposition is assumed here to be negligible.

H_2O_2 (hydrogen peroxide): Limited observations (Hall and Claiborn, 1997; Hall et al., 1999) suggest that the surface resistance for H_2O_2 is very small due to its large solubility and oxidizing capacity. Stomatal uptake is likely to be unimportant compared to the other transfer paths. The V_d for H_2O_2 should thus be higher than that of SO_2 and O_3 over most surfaces. Parameters α and β are both chosen here to be 1.

HNO_3 (nitric acid): There is extensive evidence that the surface resistance of natural surfaces to uptake of HNO_3 is effectively zero (Huebert and Robert, 1985; Harrison et al., 1989; Dollard et al., 1987; Andersen and Hovmand, 1995), so that the dry deposition of HNO_3 is controlled by aerodynamic resistances only. To avoid too high values of V_d for HNO_3, however, a small surface resistance value is assigned to HNO_3. Parameters α and β are both chosen here to be 10, which results in the surface resistance for HNO_3 having a small value under all meteorological conditions and over all surface types.

HONO (nitrous acid): Very limited data are available for HONO dry deposition. However, Harrison and Kitto (1994) measured HONO V_d values between 0.2 and $1.7\,cm\,s^{-1}$ over a grassland, and Wesely and Hicks (2000) stated that the V_d for HONO should be only slightly smaller than the V_d for HNO_3. Parameters α and β are both chosen here to be 2.0 for HONO (vs. 10.0 for HNO_3).

HNO_4 (pernitric acid): No dry-deposition data are available for this species, but it should behave similarly to HNO_3 and HONO as it also has a large solubility and is expected to have a large oxidizing capacity. Parameters α and β are both chosen here to be 5.0 for HNO_4.

NH_3 (ammonia): Although there are many measurements that we can rely on to estimate dry deposition for this species, most of these measurements were conducted in Europe. For example, Erisman et al. (1994a) found that the annual average V_d for NH_3 is $0.8\,cm\,s^{-1}$ over a heathland, almost the same as that for SO_2 (0.8–$1.0\,cm\,s^{-1}$) at the same site. However, much larger V_d values have been measured recently for some locations in Europe. Duyzer et al. (1992) found an average V_d of

3.6 cm s^{-1} over a coniferous forest. Andersen et al. (1999) found NH_3 deposition velocities as high as 20 cm s^{-1}. Sutton et al. (1992) found that the V_d of NH_3 was typically in the 1.0–4.0 cm s^{-1} range for three different moorlands. It was also found that V_d of NH_3 is much lower under frozen conditions than non-frozen conditions (Sutton et al., 1992). Examining three years of NH_3 dry-deposition flux measurements, Wyers and Erisman (1998) found that dry deposition can vary among years at the same site due to the different ambient NH_3 concentrations. At small concentrations, dry-deposition rates were observed to be smaller. At very small ambient concentration (i.e., smaller than the compensation point), emission is more important than deposition (Wyers and Erisman, 1998; Dabney and Bouldin, 1990).

The co-deposition of SO_2 and NH_3 may be important under wet conditions (Erisman and Wyers, 1993). Co-deposition of SO_2 and NH_3 enhances the dry deposition of both species whereas the resistance increases if the concentration of one or the other of these species is high and is dissolved in the water on wet surfaces, either lowering or raising the pH value. Surface resistance for NH_3 over vegetated surfaces is very sensitive to surface wetness. Surface resistances for NH_3 are close to zero over vegetated surfaces under wet conditions (Erisman et al., 1994a; Duyzer et al., 1994). Duyzer et al. (1994) suggested that NH_3 is taken up by stomata under dry conditions and by both stomata and leaf surface under less dry conditions. Even slightly high relative humidity can enhance NH_3 deposition greatly. The high deposition velocity observed in Netherland forests is mostly caused by high humidity, as explained in Erisman et al. (1994a). Such constant high humidity conditions may not exist in other areas.

Although the chemical characteristics of NH_3 are not the same as that of SO_2, they have similar deposition characteristics. Thus, NH_3 V_d is parameterized similar to SO_2. Parameters α and β are chosen here to be 1 and 0, respectively, for NH_3. No compensation point is considered due to limited knowledge at the present stage. Co-deposition is considered by changing SO_2 and NH_3 surface resistances under wet conditions based on their relative concentrations (Erisman and Wyers, 1993). If the ratio of the concentration of NH_3 to that of SO_2 is <1, the surface resistance of SO_2 is taken to be 50 s m^{-1}. If the ratio is >2.5, the surface resistance for NH_3 is taken to be 50 s m^{-1}.

PAN (peroxyacetylnitrate): Garland and Penkett (1976) found that V_d values for PAN were around 0.25 cm s^{-1} over grass and bare soil and <0.02 cm s^{-1} over water. Dry deposition for O_3 was also measured under the same conditions, yielding a PAN V_d around 50% of the O_3 V_d over grass and water surfaces, and $<20\%$ over bare soil, where the O_3 V_d was measured as 1.6 cm s^{-1} (although this value seems too large compared to other field measurements for O_3). Hill (1971) reported a value of 0.75 cm s^{-1} for the PAN V_d over an alfalfa canopy, just under 50% of the O_3 V_d at the same site. Dollard et al. (1990) studied the dry deposition of PAN to several surface types and found PAN V_d values ranging from 0.09 to 0.2 cm s^{-1}. The molecular diffusivity of PAN is smaller than that of O_3, which results in a bigger stomatal resistance for PAN than for O_3 (see Eq. (2)). Since the observed V_d for PAN is only 20–50% of that for O_3, other resistance components for PAN should be much larger than those for O_3. This also explains how the V_d for PAN can be as high as 50% of the V_d for O_3 over vegetated surfaces but only 20% over bare soil surfaces (i.e., stomatal uptake). PAN's high oxidizing capacity and relatively limited solubility also suggest that its deposition should be similar to that for O_3. Thus, parameters α and β are chosen here to be 0 and 0.6, respectively, for PAN.

PPN (peroxypropylnitrate), APAN (aromatic acylnitrate), and MPAN (peroxymethacrylic nitric anhydride): Very few (if any) observed dry-deposition data are available for these species. However, these three species do have similar chemical and physical characteristics to PAN, suggesting that they should also scale to O_3. Based on their effective Henry's law constant and pe^0(W) values, parameter α is chosen here to be 0 for all three species and β is chosen to be 0.6, 0.8, and 0.3 for PPN, APAN, and MPAN, respectively.

HCHO (formaldehyde): Very limited measurements have been made of HCHO dry deposition. Wahner and Krinke (2000) measured O_3 and HCHO dry deposition simultaneously above a deciduous forest in the summer. During nighttime V_d values were around 0.2 cm s^{-1} for O_3 and 0.5 cm s^{-1} for HCHO, and around midday V_d values were 1.1 cm s^{-1} for O_3 and 1.3 cm s^{-1} for HCHO. They also found that during rainy conditions, V_d for O_3 did not change much compared to dry conditions whereas V_d values for HCHO increased. Its relatively high solubility implies that HCHO may dry deposit similarly to SO_2. Parameters α and β are chosen here to be 0.8 and 0.2, respectively. These values will give HCHO a slightly higher V_d than O_3 and SO_2 during the day due to its larger molecular diffusivity and a smaller stomatal resistance compared to SO_2 and O_3.

MCHO (acetaldyhyde) and PALD (C3 carbonyls): No dry-deposition data are available for these two species, which have similar physical and chemical characteristics. They are not very soluble nor are they easily oxidized (propanone has been used here as a representative C3 carbonyl). For both of these two model species, parameters α and β are chosen here to be 0 and 0.05, respectively. Thus, the only effective dry-deposition pathway for these two species is via stomatal uptake.

C4A (C4–C5 carbonyls), C7A (C6–C8 carbonyls), ACHO (aromatic carbonyls), MVK

(methyl-vinyl-ketone), and MACR (methacrolein): No dry-deposition data are available for these five species, which have similar chemical and physical characteristics and are assumed here to have the same α and β values. These species are not very soluble, nor do they have a high oxidizing capacity (butyraldehyde and 2-butanone have been considered as representative C4–C5 carbonyls (i.e., one aldehyde, one ketone), heptanal and heptanone as representative C6–C8 carbonyls, and benzaldehyde as a representative aromatic carbonyl). For all five model species, parameters α and β are chosen here to be 0 and 0.05, respectively.

MGLY (methylgloxal): No dry-deposition data are available for this species, which is just slightly soluble. Thus, α and β are chosen here to be 0.01 and 0, respectively.

MOH (methyl alcohol), ETOH (ethyl alcohol), and POH (C3 alcohols): No dry-deposition data are available for these three species, which have similar chemical and physical characteristics and are discussed together. However, Chamel and Gambonnet (1997) found that sorption and transfer of an ethoxylated stearic alcohol into and through isolated tomato and pepper cuticles was rapid at low concentrations. These three species are soluble but not very reactive. Based on their H^* and pe^0(W) values, parameters α and β are chosen here to be 0.6 and 0.1, respectively, for MOH, 0.6 and 0, respectively, for ETOH, and 0.4 and 0, respectively, for POH.

CRES (cresol): No dry-deposition data are available for this species, which is slightly soluble and has a very small oxidizing capacity. Parameters α and β are chosen here to be 0.01 and 0, respectively.

FORM (formic acid) and ACAC (acetic acid): Hartmann et al. (1991) estimated dry-deposition velocities from observed concentration data for formic acid and acetic acid. V_d values over a scrub-grass savannah area were $1.0 \pm 0.3\,\mathrm{cm\,s^{-1}}$ for both FORM and ACAC during the rainy season. For the dry season, V_d was estimated to be $0.64 \pm 0.2\,\mathrm{cm\,s^{-1}}$ for FORM and $0.5 \pm 0.2\,\mathrm{cm\,s^{-1}}$ for ACAC. Sanhueza et al. (1992) reported V_d values of $1.1 \pm 0.6\,\mathrm{cm\,s^{-1}}$ and $0.68 \pm 0.42\,\mathrm{cm\,s^{-1}}$ for FORM and ACAC, respectively, for dewy conditions over a forest area. Considering that these two species are very soluble, they should dry deposit like SO_2, with their V_d values probably slightly higher than those for SO_2. Parameters α and β are chosen here to be 2.0 and 0, respectively, for FORM, and 1.5 and 0, respectively, for ACAC.

ROOH (organic peroxides): Hall and Claiborn (1997) and Hall et al. (1999) observed dry-deposition velocities of ROOH over forests and obtained a typical value of $1.6\,\mathrm{cm\,s^{-1}}$ for the day and $0.5\,\mathrm{cm\,s^{-1}}$ at night. They estimated a surface resistance for ROOH of about $15\,\mathrm{s\,m^{-1}}$ over a pine forest and 20–$40\,\mathrm{s\,m^{-1}}$ over a deciduous forest. These values seem a bit small. Considering methyl hydroperoxide as a representative species, this VOC group has a large solubility range, depending on environmental conditions, and its pe^0(W) value suggests that it has some oxidizing capacity, although not as high as O_3. Parameters α and β are chosen here to be 0.1 and 0.8, respectively.

ONIT (organic nitrates) and INIT (isoprene nitrate): No dry-deposition data have been located for these two species. Based on their similar chemical and physical characteristics, these two species will be assumed to have the same α and β values. Their deposition should be similar to PAN according to their solubility and reactivity (methyl nitrate has been considered as a representative organic-nitrate species). Parameters α and β are chosen here to be 0 and 0.5, respectively, for both species.

All of the α and β values discussed above are listed in Table 1. For all species, especially those with small surface resistances, a lower limit of $10\,\mathrm{s\,m^{-1}}$ is chosen for surface resistance to avoid too large V_d values. Knowledge of two other parameters, leaf area index LAI (see Eqs. (5)–(7) and (9)) and aerodynamic roughness length z_0 (for R_a and R_b), is needed to estimate V_d. Values for these two parameters are either taken from our previous studies (Brook et al., 1999; Zhang et al., 2001b) or from related references (Dorman and Sellers, 1989; Meeson et al., 1995; Sellers et al., 1996). The values adopted for these two parameters are listed in Table 2 for each of the 15 LUCs and 5 SCs.

3. Evaluation

3.1. Evaluation using O_3 and SO_2 observations

There are a number of O_3 and SO_2 dry-deposition data sets available to us, and these data sets have been used to evaluate the scheme's performance for the base species. The five flux and concentration data sets available for O_3 are for a deciduous-forest (LUC 4) site in Ontario, Canada (Borden) from July 7 to August 30, 1988 (Padro et al., 1991) and from March 17 to April 26, 1990 (Padro et al., 1992), a mixed-forest (LUC 5) site in New York state, USA (Sand Flats) from May 12 to October 20, 1998 (Finkelstein et al., 2000), a grassland (LUC 6) site in northeastern Colorado, USA from June 23 to July 12, 1988 (Padro et al., 1998), and a vineyard-field (LUC 7) site in the San Joaquin Valley, California, USA from July 11 to August 5, 1991 (Massman et al., 1994). The two flux and concentration data sets available for SO_2 are for a deciduous-forest (LUC 4) site in Ontario, Canada (Borden) from March 17 to April 26, 1990 (Padro et al., 1992) and a mixed-forest (LUC 5) site in New York state, USA (Sand Flats) from May 12 to October 20, 1998 (Finkelstein et al., 2000). The site measurements of meteorological variables are

used for the evaluations. Observed site-specific LAI is also used for the evaluation since the scheme is very sensitive to this parameter, and the default LAI values given in Table 2 may differ greatly from those at particular sites. LAI values are available every half hour for the Sand Flats site (Finkelstein et al., 2000). LAI was estimated to be 5.0, 0.5, 1.0 and 3.0 for the summer Borden forest, winter Borden forest, Colorado grassland, and San Joaquin Valley vineyard, respectively (Padro, 1996). All other parameters needed are taken from the default values listed in Table 2.

Fig. 1 shows scatterplots of the O_3 V_d values inferred from measurements versus modelled values for the five O_3 dry-deposition data sets. Fig. 2 compares composited observed and predicted diurnal cycles for O_3 V_d based on half-hourly averages for the same five data sets, and Table 3 presents the statistical results of the comparison. For a deciduous-forest site in the summer (SC 1), modelled results are in good agreement with measurements (Fig. 1), with a correlation coefficient of 0.67. However, the model does not predict the higher V_d values (i.e., over $1.3\,cm\,s^{-1}$). The averaged modelled nighttime V_d values are slightly lower than the measured values (Fig. 2), implying that the parameterization for non-stomatal uptake is slightly smaller at this site than it should be. In the morning, the stomata open rapidly, resulting in the daily maximum V_d values occurring before noon, and the model cannot capture this phenomenon. For a deciduous-forest site in the winter (SC 4), the model does not perform very well, and neither the correlation coefficient (0.37) nor the predicted average diurnal cycle are satisfactory. In the winter season, the frequency of wet canopies is usually higher than in summer. Difficulties in measuring and modelling canopy wetness could be one reason for this unsatisfactory model performance in the winter season, especially for observed higher V_d values. Also, the estimated LAI values and other canopy characteristics may cause errors in predicted dry-deposition velocities. However, the average V_d values from model and measurements for the wintertime deciduous forest are very close (Table 3). For a mixed-forest site, the modelled V_d values agree broadly with the measurements (Fig. 1), although the correlation coefficient is only 0.58. Comparison of the observed and predicted diurnal cycles (Fig. 2) for this data set suggests that the model slightly underestimates the O_3 V_d during the early morning but overestimates it in the afternoon.

For the summertime grassland site data set, the modelled V_d values seem to lie within a reasonable range compared to the measurements (Fig. 1), except for a few very high observed V_d values. At this site, NO emissions from the soil were high and chemical reactions affected O_3 dry deposition to a small extent (Padro et al.,

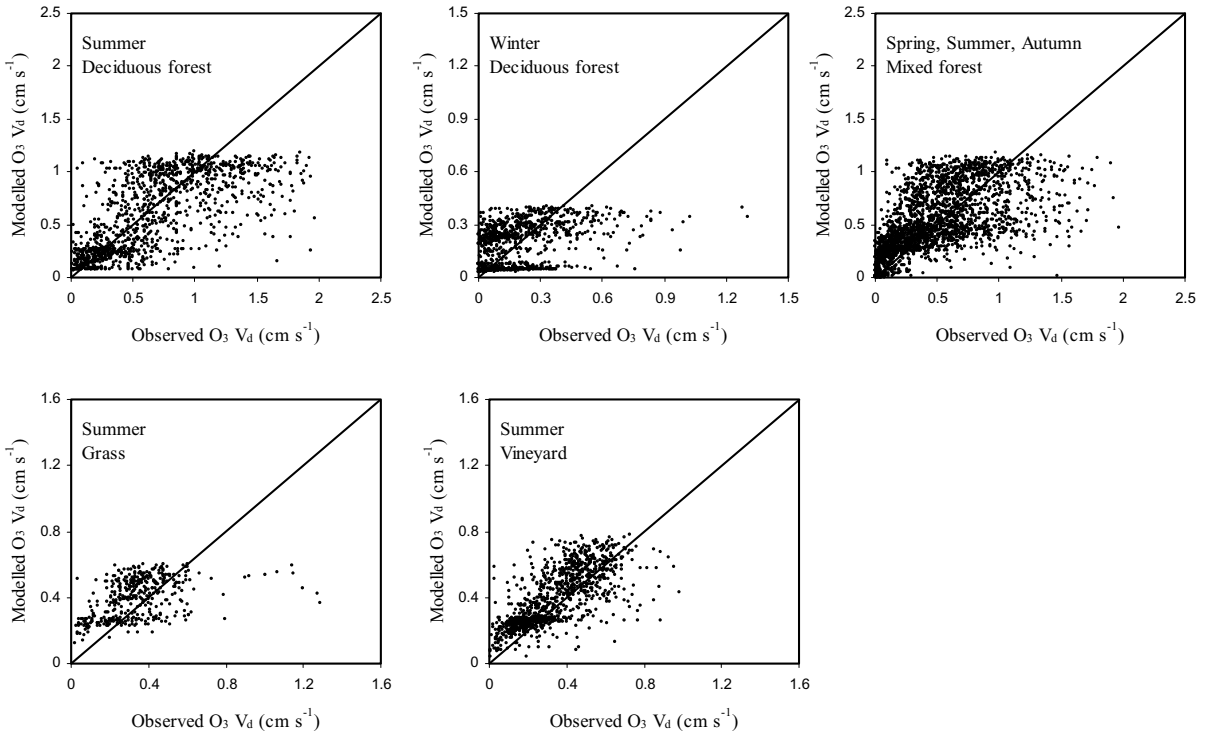

Fig. 1. Scatterplots of observed vs. predicted O_3 dry-deposition velocities for five different dry-deposition data sets.

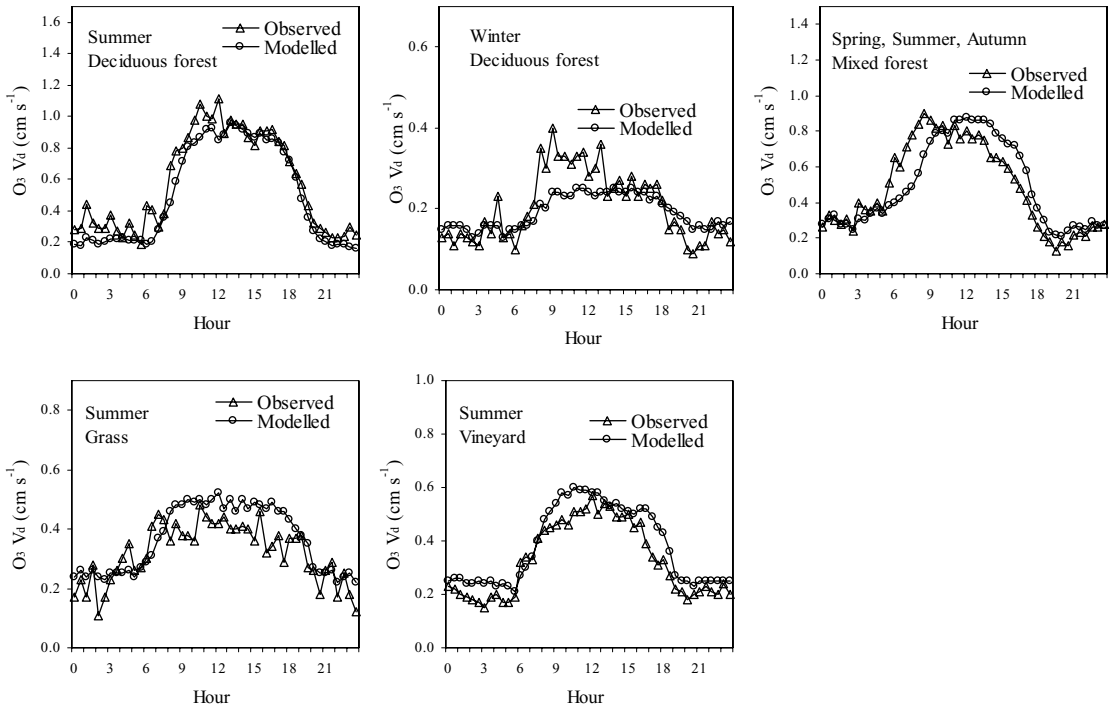

Fig. 2. Comparison of average diurnal time series of observed vs. predicted O_3 dry-deposition velocities for five different dry-deposition data sets.

Table 3
Statistical results of modelled and observed dry-deposition velocities for O_3 and SO_2[a]

	V_{do}	V_{dm}	R	N	Period
O_3 deciduous forest	0.67 ± 0.45	0.60 ± 0.36	0.67	1168	7 July–30 August, 1988
O_3 deciduous forest	0.21 ± 0.18	0.20 ± 0.12	0.37	875	17 March–26 April, 1990
O_3 mixed forest	0.50 ± 0.36	0.54 ± 0.30	0.58	2283	12 May–20 October, 1998
O_3 grassland	0.34 ± 0.19	0.40 ± 0.12	0.44	399	23 June–12 July, 1988
O_3 vineyard	0.33 ± 0.18	0.38 ± 0.17	0.72	1120	11 July–5 August, 1991
SO_2 deciduous forest	0.48 ± 0.45	0.38 ± 0.15	0.43	238	17 March–26 April, 1990
SO_2 mixed forest	0.86 ± 0.53	0.74 ± 0.30	0.57	150	12 May–20 October, 1998

[a] Note: V_{do} is observed mean $\pm$ standard deviation of V_d; V_{dm} is modelled mean $\pm$ standard deviation of V_d; R is the correlation coefficient between observed and modelled V_d; and N is the number of observed data samples.

1998). This may be one reason for the small correlation coefficient (0.44) between the model results and measurements. Examination of the average diurnal cycle (Fig. 2) suggests that the model slightly overestimates O_3 V_d for most of the day. Finally, for the summertime vineyard site data set, the model seems to perform very well. The difference between modelled and observed V_d is small (Fig. 1) and the correlation is high (0.72). Comparison of the average diurnal cycles for this data set suggests that the model slightly overestimates O_3 V_d for most of the day. This may be caused by the parameterization of non-stomatal uptake, such as a too small soil resistance.

The averaged modelled O_3 V_d values for all five data sets are within 20% of the averaged measurements (Table 3). Compared to other big-leaf models (Padro et al., 1991, 1992, 1998; Massman et al., 1994) and to multi-layer models (Finkelstein et al., 2000) that considered the same data sets used here, the current model gives better results. Given that the results shown here are based on the default parameters (except LAI) listed in Table 2, we conclude that the current model can

predict reasonable O_3 V_d values for different LUCs and seasons.

Fig. 3 provides a graphical comparison of SO_2 V_d predictions with measurements for two sites. The corresponding statistical results are listed in Table 3. For the deciduous-forest site in the winter (SC 4), the modelled SO_2 V_d underpredicts all observed values $>0.8\,cm\,s^{-1}$. Again, one reason for this may be difficulties in measuring and modelling canopy wetness. For the mixed-forest-site data set, most of the measurements were made under dry conditions and the scheme seems to perform better than for the wintertime deciduous forest data set. However, the scatterplots for both data sets indicate that the measured SO_2 V_d values have a larger range than the modelled values. Note that for the comparison of average diurnal cycle, there is just one sample for both the 0:30 LST and 7:00 LST half-hour periods, when the measured V_d values are much higher than the modelled values. The measurement error for SO_2 is expected to be larger than for O_3 due to the smaller ambient concentrations of SO_2. The average modelled V_d values for SO_2 is within a 30% range compared to measurements (Table 3).

3.2. Example modelled dry-deposition velocities

As already mentioned, there are no data available to evaluate the scheme for most of the dry-depositing species considered. Instead, example modelled dry-deposition velocities have been calculated for all 31 dry depositing species for different environmental conditions and these values have been compared with the available dry-deposition measurements discussed in Section 2.4.2.

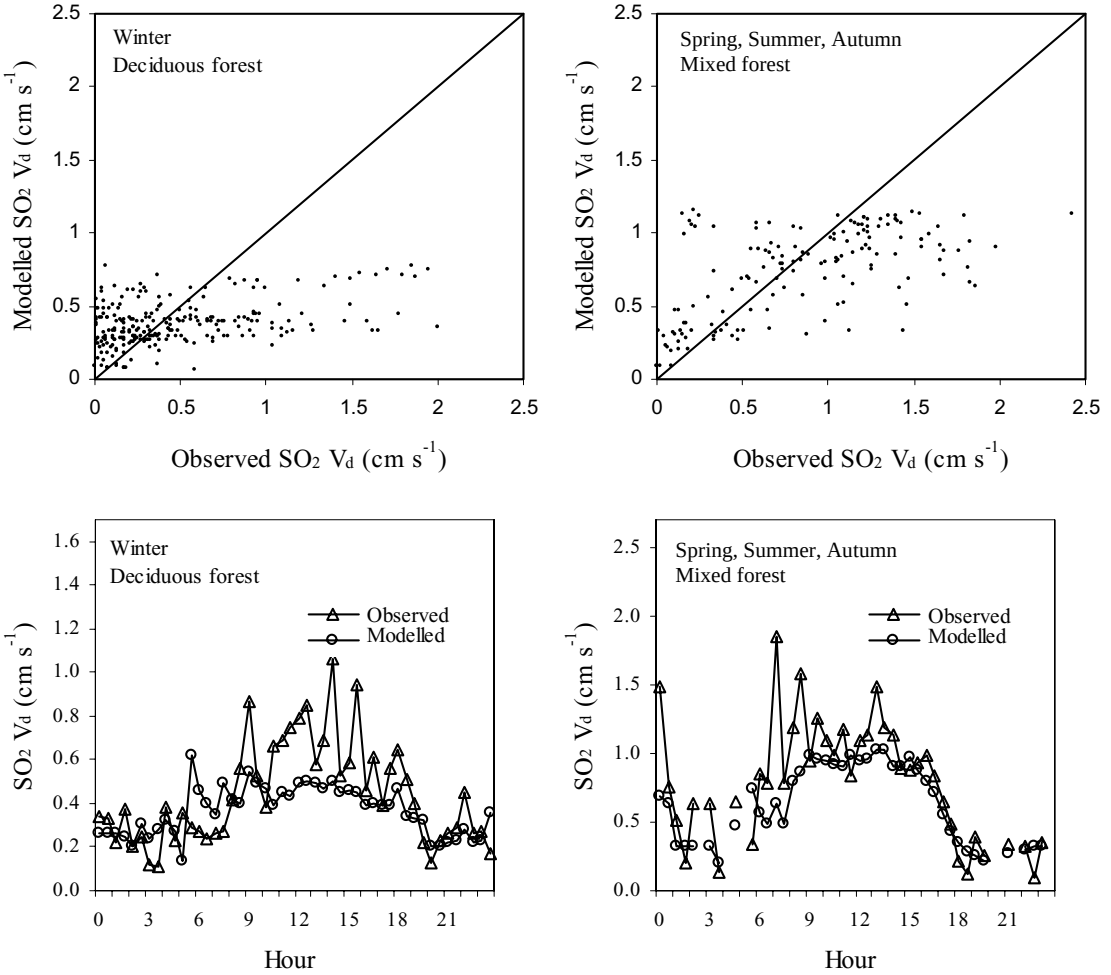

Fig. 3. Scatterplots of observed vs. predicted SO_2 dry-deposition velocities and average diurnal time series of observed vs. predicted O_3 dry-deposition velocities for two different data sets.

Table 4 lists modelled V_d values for all species and all LUCs for a typical dry summer daytime condition. The reference height for calculating V_d is taken as 10 m. The solar irradiation is chosen to be 800 W m^{-2}. The wind speed and temperature at 10 m is taken to be 8 m s^{-1} and 290 K, respectively. It is evident from Table 4 that canopies having larger LAI values and smaller minimum stomatal resistances (LUC 1–7) have higher V_d values for stomatally controlled species such as O_3, NO_2, PAN, PPN, ROOH, and ONIT. Wet surfaces (LUC 11–14) have higher V_d values for soluble species (e.g., SO_2, FORM, ACAC, NH_3). Canopies with bigger roughness lengths (LUC 1–5) have higher V_d values for species with small surface resistances (e.g., HNO_3, HNO_4, HONO). Those species with relatively limited solubility and little oxidizing capacity (MCHO, PALD, C4A, C7A, ACHO, MVK, MACR) have V_d values close to zero over unvegetated surfaces (i.e., LAI values of zero), since the primary deposition pathway for these species is stomatal uptake.

During winter (table and figure are not shown here), canopies with evergreen tree species (LUC 1, 2, and 5) can still remove gaseous pollutants by dry deposition at temperatures which are not too low (i.e., above the minimum temperature threshold T_{min} at which stomata start opening). Those gaseous species with higher solubilities (e.g., SO_2, FORM, ACAC, NH_3) can have higher V_d values compared to other species because it is often wet in winter. Species with relatively limited solubility and very low oxidizing capacity, on the other hand, have very low V_d values in the winter over most canopies (except evergreen trees). Note that when predicted V_d values are compared with the available measurements reviewed in Section 2, the modelled values are found to be within the range of measurements for those species for which some data are available.

Fig. 4 shows one example of the sensitivity by species of dry deposition to environmental conditions. It is for a deciduous broadleaf forest (LUC 4) for the summer season (SC 1) for four sets of conditions: a typical day and night with and without rain. A solar irradiation value of 600 W m^{-2} is assumed for the daytime conditions. Under the same wetness conditions, daytime V_d values are higher than nighttime values for all species

Table 4
Modelled dry-deposition velocities (cm s^{-1}) for summer daytime conditions

	LUC													
	1	2	3	4	5	6	7	8	9	10	11	12	13/14	15
Species					Summer	Daytime	($R_s = 800$ W m^{-2})	$T = 290$ K	$U = 8$ m s^{-1}					
SO_2	0.819	0.938	0.468	0.89	1.079	0.632	0.583	0.147	0.235	0.366	1.292	0.723	1.076	0.259
H_2SO_4	0.995	1.099	0.685	1.041	1.212	0.812	0.776	0.330	0.339	0.572	1.313	0.741	1.054	0.456
NO_2	0.799	0.812	0.419	0.885	1.099	0.603	0.546	0.162	0.099	0.336	0.132	0.041	0.04	0.224
O_3	0.841	0.852	0.466	0.923	1.136	0.646	0.59	0.2	0.122	0.381	0.153	0.051	0.05	0.265
H_2O_2	1.231	1.356	0.775	1.318	1.571	0.957	0.899	0.334	0.343	0.627	1.372	0.76	1.112	0.481
HNO_3	4.558	6.092	4.104	4.7	5.042	2.967	2.956	1.856	1.812	2.679	2.587	2.065	1.207	3.382
HONO	1.668	1.899	1.237	1.728	1.969	1.321	1.28	0.613	0.624	1.002	1.958	1.176	1.227	0.869
HNO_4	2.872	3.524	2.455	2.92	3.175	2.118	2.099	1.219	1.215	1.817	2.545	1.718	1.191	1.914
NH_3	1.211	1.365	0.614	1.351	1.675	0.875	0.791	0.149	0.237	0.455	1.36	0.743	1.142	0.298
PAN	0.549	0.552	0.295	0.604	0.748	0.426	0.387	0.122	0.074	0.242	0.095	0.031	0.03	0.163
PPN	0.531	0.533	0.289	0.584	0.721	0.415	0.377	0.122	0.074	0.238	0.094	0.031	0.03	0.162
APAN	0.541	0.537	0.324	0.583	0.707	0.438	0.405	0.16	0.098	0.277	0.113	0.04	0.04	0.199
MPAN	0.436	0.442	0.206	0.49	0.62	0.326	0.288	0.062	0.038	0.159	0.06	0.016	0.015	0.097
HCHO	1.004	1.116	0.535	1.108	1.365	0.748	0.681	0.159	0.214	0.41	1.163	0.627	1.057	0.278
MCHO	0.386	0.395	0.19	0.422	0.489	0.301	0.267	0.011	0.007	0.134	0.048	0.003	0.003	0.063
PALD	0.359	0.367	0.173	0.394	0.459	0.278	0.246	0.011	0.007	0.122	0.043	0.003	0.003	0.057
C4A	0.338	0.346	0.161	0.372	0.436	0.261	0.230	0.011	0.007	0.113	0.040	0.003	0.003	0.053
C7A	0.286	0.292	0.132	0.317	0.377	0.219	0.192	0.011	0.007	0.093	0.032	0.003	0.003	0.044
ACHO	0.303	0.309	0.141	0.335	0.396	0.232	0.204	0.011	0.007	0.099	0.035	0.003	0.003	0.047
MVK	0.499	0.517	0.188	0.579	0.752	0.345	0.292	0.011	0.007	0.125	0.041	0.003	0.003	0.056
MACR	0.341	0.348	0.162	0.375	0.439	0.263	0.232	0.011	0.007	0.114	0.040	0.003	0.003	0.054
MGLY	0.483	0.503	0.176	0.562	0.733	0.331	0.278	0.002	0.003	0.113	0.055	0.010	0.049	0.046
MOH	0.897	0.988	0.446	1.002	1.249	0.658	0.591	0.110	0.157	0.334	0.948	0.497	0.969	0.213
ETOH	0.771	0.856	0.383	0.860	1.072	0.570	0.511	0.090	0.145	0.287	0.929	0.491	0.955	0.182
POH	0.473	0.519	0.274	0.503	0.573	0.385	0.354	0.061	0.098	0.210	0.680	0.348	0.816	0.131
CRES	0.412	0.429	0.150	0.480	0.627	0.284	0.238	0.002	0.003	0.097	0.050	0.010	0.049	0.040
FORM	1.194	1.423	0.770	1.268	1.492	0.933	0.883	0.284	0.441	0.609	1.910	1.145	1.228	0.473
ACAC	0.985	1.156	0.611	1.053	1.251	0.772	0.725	0.217	0.340	0.485	1.635	0.954	1.163	0.364
ROOH	0.819	0.842	0.443	0.902	1.114	0.624	0.568	0.176	0.122	0.357	0.309	0.134	0.390	0.244
ONIT	0.459	0.456	0.276	0.486	0.556	0.381	0.352	0.103	0.062	0.226	0.089	0.026	0.026	0.148
INIT	0.402	0.397	0.244	0.425	0.490	0.336	0.311	0.102	0.062	0.204	0.082	0.026	0.025	0.138

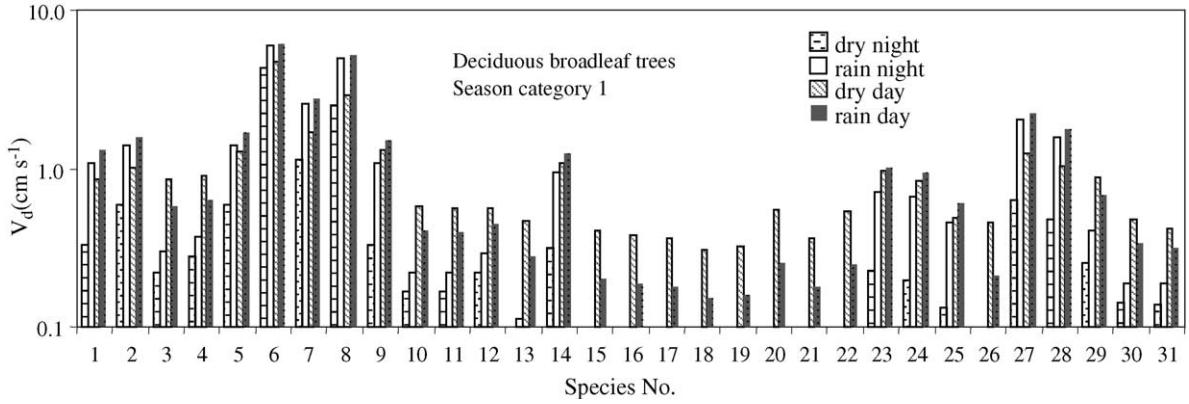

Fig. 4. Histograms of predicted dry-deposition velocities for 31 AURAMS species for four different sets of environmental conditions (daytime with and without precipitation, nighttime with and without precipitation) for a deciduous broadleaf forest in summer.

due to the contribution of sunlight-dependent stomatal uptake. For those species with small surface resistances (e.g., HNO_3, HNO_4, HONO), the differences between daytime and nighttime V_d values are not as big as for other species. For those species with very relatively limited and very low oxidizing ability (e.g., MCHO, PALD, C4A, MACR), nighttime V_d values are close to zero due to stomatal closure. During nighttime, wetness due to rain slightly increases V_d values for not very soluble species (e.g., NO_2, O_3, PAN) but greatly increases V_d values for soluble species (e.g., SO_2, NH_3, FORM). During daytime, wetness due to rain also increases V_d for those species with higher solubility, though not to the same degree. For not very soluble species, on the other hand, wetness due to rain decreases V_d in this example due to partial stomatal closure. Under dry conditions with weak solar radiation, however, when V_d is expected to be small, then rain can actually increase V_d values even for species with very small solubilities. Overall, V_d for most species can be higher than $0.5\,cm\,s^{-1}$ during the daytime and above $5\,cm\,s^{-1}$ for several species with very high solubility and oxidizing capacity.

4. Summary

A parameterization scheme for gaseous dry-deposition velocities has been developed for AURAMS, a new regional air-quality model with 48 transported gas-phase species for which dry deposition must be considered. Aerodynamic and quasi-laminar sublayer resistances are estimated by standard formulations. Two approaches have been used to estimate the various surface resistance components for 31 different chemical species, 15 LUCs, and 5 SCs: a "two-big-leaf" canopy stomatal resistance submodel is used to estimate time-of-day-dependent canopy stomatal resistance and look-up tables are used to specify for mesophyll, dry-ground, wet-ground, dry-cuticle, and wet-cuticle resistances. Five categories of surface wetness are considered: dry; highly humid; wetted by dew; wetted by rain; and snow-covered.

Two species, SO_2 and O_3, are used as base species to scale the dry-deposition rates for other chemical species. Both published dry-deposition data and measurements and/or estimates of aqueous solubility and oxidizing capacity have been employed in this scheme to specify dry-deposition velocities for other chemical species. First, values of effective Henry's law constant and electron activity for half-redox reactions in neutral aqueous solutions are ranked to separate the 48 AURAMS transported species into a group of 31 species for which dry deposition is likely to be a significant process and a second group of 17 species for which dry deposition is likely to be unimportant (not shown in Table 1). Second, scaling parameters relative to the two base species are chosen for the 29 other AURAMS dry-depositing species through consideration of published dry-deposition data, tabulated aqueous solubility and oxidizing capacity values, and chemical structure of the chemical species. The scaling parameter values that have been chosen, especially for those species without observational data, unavoidably are somewhat subjective, and they may require adjustment as more observational data become available and our understanding on dry deposition improves.

Evaluations using five O_3 and two SO_2 dry-deposition data sets and some example predictions for all species over different environmental conditions suggest that this scheme can predict reasonable dry-deposition velocities for the 31 AURAMS gaseous species considered to dry deposit and is suitable for air-quality modelling.

However, the scheme needs further evaluation for those species with very limited measurement data. It would be valuable to have more dry-deposition measurements of any of the species under a wider range of conditions, including different land cover and vegetation types, different seasons, and different weather conditions. Other improvements will likely be required as our understanding of dry deposition, the level of complexity of air quality model meteorology, and the level of complexity of land use data improves. The effect of canopy wetness and soil moisture on dry deposition, and the role of compensation point on dry deposition are likely candidates for future improvements.

Acknowledgements

We greatly appreciate very helpful discussions with Dr. Marvin Wesely during the course of this work. Comments from others in the AURAMS group—Wanmin Gong, Ashu Dastoor, Veronique Bouchet, Balbir Pabla—and constant support from the manager of this project, Dr. Srinivasan Venkatesh, are also greatly appreciated. This work has been financially supported by Air Quality Research Branch of the MSC.

Appendix A. Calculation of effective Henry's Law values

The effective Henry's Law constant (H^*) allows for other aqueous equilibria to be included in the expression for gas/aqueous-phase equilibrium for a compound. For example, gas-phase nitric acid will be in equilibrium with the aqueous-phase nitric acid, and the latter will also be in equilibrium with H^+ and NO_3^-, its two dissociation products (Herrmann et al., 1999; Seinfeld and Pandis, 1998):

$$HNO_3(g) \Leftrightarrow HNO_3(aq),\ H_{HNO_3} = 2.1\times10^5\ \mathrm{M\ atm^{-1}}$$

(Herrmann et al., 1999)

$$HNO_3(aq) \Leftrightarrow H^+ + NO_3^-,\ K = 15.4\ \mathrm{M}$$

(Seinfeld and Pandis, 1998).

The H^* value describes the equilibrium between the gas-phase and the total aqueous-phase concentration. In the above case, this may be defined as the total nitrate in solution, TN, where

$$[TN] = [HNO_3(aq)] + [NO_3^-].$$

The above equilibrium reactions can be translated into the following equations:

$$[HNO_3(aq)] = H_{HNO_3}\ P_{HNO_3}$$

$$K[HNO_3(aq)] = [H^+][NO_3^-],$$

where H_{HNO_3} is the Henry's Law constant for HNO_3, P_{HNO_3} is the gas-phase partial pressure of HNO_3, and K is the equilibrium constant for aqueous-phase dissociation of HNO_3. Then

$$[NO_3^-] = K[HNO_3(aq)]/[H^+],$$

$$[TN] = [HNO_3(aq)]\{1 + K/[H^+]\}$$

and substitution into the original gas–aqueous phase equilibrium equation gives

$$[TN] = H_{HNO_3} P_{HNO_3}\{1 + K/[H^+]\}.$$

The expression $H_{HNO_3}\ \{1+K/[H^+]\}$ is the effective Henry's Law constant, which describes the equilibrium between gas-phase HNO_3 and the total nitrate in the aqueous phase. Neutral water is used ($[H^+] = 10^{-7}$ M), so that the H^* values are relative to neutral water.

Similar expressions can be derived for other gas-phase species for which dissociation in the aqueous phase is known to occur. Table 5 gives the Henry's Law values, (gas $\Leftrightarrow$ aqueous-phase equilibrium), the known dissociation reactions, the resulting expression for H^*, and the H^* values themselves for various gas-phase species considered in this paper. Note that a number of VOCs in the AURAMS mechanism are not listed in the table; these have very low H values and are not considered to have a significant presence in the aqueous or dissociated phases.

Appendix B. Example pe^0(W) values for various half-redox reactions

The pe^0(W) value of a half-redox reaction is the negative base ten logarithm of its electron activity for a neutral aqueous solution. This is a measure of its oxidizing capability or intensity relative to the neutral solution.

The value of pe^0(W) is given by (Stumm and Morgan (1996)):

$$pe^0(W) = \frac{1}{n}\left[\log_{10}(K)\right] + \frac{n_H}{2}\left[\log_{10}(K_W)\right],$$

where K is the equilibrium constant of the reduction half-reaction, K_w is the equilibrium constant for water dissociation, n is the number of electrons in the half-reaction, and n_H is the number of protons exchanged per electron in the half-reaction. Activity coefficients of unity are assumed, the solution pH is assumed to be 7, and the value of K_w at 298 K (i.e., $10^{-14}\ \mathrm{M^2}$) is used, resulting in the equation

$$pe^0(W) = \frac{1}{n}\left[\log_{10}(K)\right] - 7\,n_H.$$

The first part of this equation is the negative base ten logarithm of the electron activity at equilibrium and

Table 5
Henry's Law and effective Henry's Law values for AURAMS species[a]

Species	H ($M\,atm^{-1}$)	Dissociation reactions	H^* expression	H^* value ($M\,atm^{-1}$)	Data source(s)
SO_2	$H_{SO_2} = 1.23$	$SO_2(g) + H_2O \Leftrightarrow SO_2 \cdot H_2O(aq)$, H_{SO_2}	$[S(IV)] = H_{SO_2}\, P_{SO_2}\left[1 + \frac{K_1}{[H^+]} + \frac{K_1K_2}{[H^+]^2}\right]$	2.65×10^5	1
		$SO_2 \cdot H_2O(aq) \Leftrightarrow H^+(aq) + HSO_3^-(aq)$, K_1	$K_1 = 1.3 \times 10^{-2}$ M		
		$HSO_3^-(aq) \Leftrightarrow H^+(aq) + SO_3^{2-}(aq)$, K_2	$K_2 = 6.6 \times 10^{-8}$ M		
H_2SO_4	$H_{H_2SO_4}$ assumed "very large"	$H_2SO_4(g) \Leftrightarrow H_2SO_4(aq)$, $H_{H_2SO_4}$	$[S(VI)] = H_{H_2SO_4}\, P_{H_2SO_4}\left[1 + \frac{K_1}{[H^+]} + \frac{K_1K_2}{[H^+]^2}\right]$	$H^*_{H_2SO_4}$ V. large	2
		$H_2SO_4(aq) \Leftrightarrow H^+ + HSO_4^-$, K_1			
		$HSO_4^- \Leftrightarrow H^+ + SO_4^=$, K_2			
NO	$H_{NO} = 1.9 \times 10^{-3}$	No dissociation	$H^*_{NO} = H_{NO}$	1.9×10^{-3}	1
NO_2	$H_{NO_2} = 1.2 \times 10^{-2}$	No dissociation. Aqueous removal reactions known	$H^*_{NO_2} = H_{NO_2}$	1.2×10^{-2}	2
O_3	$H_{O_3} = 1.14 \times 10^{-2}$	No dissociation. Aqueous removal reactions known	$H^*_{O_3} = H_{O_3}$	1.14×10^{-2}	2
H_2O_2	$H_{H_2O_2} = 1.02 \times 10^5$	No dissociation. Aqueous removal reactions known	$H^*_{H_2O_2} = H_{H_2O_2}$	1.02×10^5	2
HNO_3	$H_{HNO_3} = 2.1 \times 10^5$	$HNO_3(g) \Leftrightarrow HNO_3(aq)$, H_{HNO_3}	$[TN] = H_{HNO_3}\, P_{HNO_3}\, \{1 + K/[H^+]\}$	3.23×10^{13}	1, 2
		$HNO_3(aq) \Leftrightarrow H^+ + NO_3^-$, K	$K = 15.4$ M		
HONO	$H_{HONO} = 49$	$HONO(g) \Leftrightarrow HONO(aq)$, H_{HONO}	$[TN] = H_{HONO} P_{HONO}\, \{1 + K/[H^+]\}$	2.6×10^5	2
		$HONO(aq) \Leftrightarrow H^+ + NO_2^-$, K	$K = 5.3 \times 10^{-3}$ M		
HNO_4	$H_{HNO_4} = 1 \times 10^5$	$HNO_4(g) \Leftrightarrow HNO_4(aq)$, H_{HNO_4}	$[\text{Total Aq. N}] = H_{HNO_4}\, P_{HNO_4}\left\{1 + \frac{K_1}{[H^+(aq)]} + \frac{K_2}{[HO_2(aq)]}\right\}$	1×10^7 (lower limit, if $[HO_2(aq)]$ small)	2
		$HNO_4(aq) \Leftrightarrow H^+ + ONO_2^-$, K_1	$K_1 = 1 \times 10^{-5}$ M		
		$HO_2NO_2(aq) \Leftrightarrow NO_2(aq) + HO_2(aq)$, K_2	$K_2 = 4.6 \times 10^{-10}$ M		
NH_3	$H_{NH_3} = 60.7$	$NH_3(g) \Leftrightarrow NH_3(aq)$, H_{NH_3}	$[\text{Total Ammonia/um}] = H_{NH_3}\, P_{NH_3}\left\{1 + \frac{K_1[H^+]}{K_{H_2O}[H_2O]}\right\}$	1.1×10^4	2
		$NH_3(aq) + H_2O \Leftrightarrow NH_4^+(aq) + OH^-(aq)$	$K_1 = 1.77 \times 10^{-5}$ M		
		$H_2O \Leftrightarrow H^+(aq) + OH^-(aq)$; K_{H_2O}	$K_{H_2O} = 1.8 \times 10^{-16}$		
PAN	$H_{PAN} = 5$	No dissociation	$H^*_{PAN} = H_{PAN}$	5	2
PPN	$H_{PPN} = 2.9$	No dissociation	$H^*_{PPN} = H_{PPN}$	2.9	7
APAN	No data, but expected to be similar to PAN	No dissociation	$H^*_{APAN} = H_{PAN}$	5	
MPAN	$H_{MPAN} = 1.7$	No dissociation	$H^*_{MPAN} = H_{MPAN}$	1.7	7
HCHO	$H_{HCHO} = 2.5$	$HCHO(g) \Leftrightarrow HCHO(aq)$, H_{HCHO}	$H^*_{HCHO} = H_{HCHO}\, \{1 + K_1[H_2O]\}$	4.9×10^3	1, 2
		$HCHO(aq) + H_2O \Leftrightarrow CH_2(OH)_2(aq)$, K_1	$K_1 = 35.2\,M^{-1}$, $[H_2O] = 55.5$ M		
MCHO	$H_{MCHO} = 15$	No dissociation. Aqueous removal reactions known	$H^*_{MCHO} = H_{MCHO}$	15	3
PALD	$H_{PALD} = 32$	Dissociation unknown	$H^*_{PALD} = H_{PALD}$	32	3
C4A	$H_{C4A} = 8.7 - 17.6$	Dissociation unknown	$H^*_{C4A} = H_{C4A}$	17.6	3
C7A	$H_{C7A} = 3.7 - 110$	Dissociation unknown	$H^*_{C7A} = H_{C7A}$	110	3

ACHO	No data available	Group method estimate used	$H^*_{ACHO} = H_{ACHO}$	37.4	4
MVK	No data available	Group method estimate used	$H^*_{MVK} = H_{MVK}$	38.3	5
MACR	No data available	Group method estimate used	$H^*_{MACR} = H_{MACR}$	3.5	5
MGLY	$H_{MGLY} = 3.7 \times 10^3$	Dissociation unknown	$H_{MGLY} = H^*_{MGLY}$	3.7×10^3	3
MOH	$H_{MOH} = 2.2 \times 10^2$	No dissociation. Aqueous removal reactions known	$H^*_{MOH} \geqslant H_{MOH}$	2.2×10^2	2
ETOH	$H_{ETOH} = 1.9 \times 10^2$	No dissociation. Aqueous removal reactions known	$H^*_{ETOH} \geqslant H_{ETOH}$	1.9×10^2	2
POH	$H_{POH} = 1.3 \times 10^2$	No dissociation. Aqueous removal reactions known	$H^*_{POH} \geqslant H_{POH}$	1.3×10^2	7
CRES	$H_{CRES} = 8.3 \times 10^2$	Dissociation unknown	$H^*_{CRES} = H_{CRES}$	8.3×10^2	3
FORM	$H_{FORM} = 5.5 \times 10^3$	$HCOOH(g) \Leftrightarrow HCOOH(aq)$, H_{FORM} $HCOOH(aq) \Leftrightarrow HCOO^- + H^+$, K	$[\text{Total Formate}] = H_{HCOOH}\, P_{HCOOH} \left\{1 + \frac{K}{[H^+]}\right\}$ $K = 1.77 \times 10^{-4}$ M	9.8×10^6	2
ACAC	$H_{ACAC} = 5.5 \times 10^3$	$ACAC(g) \Leftrightarrow ACAC(aq)$, $H_{CH_3C(O)OH}$ $ACAC(aq) \Leftrightarrow CH_3C(O)O^-(aq) + H^+(aq)$; K_1	$[\text{Total Aq. Acetate}] = H_{ACAC}\, P_{ACAC} \left\{1 + \frac{K_1}{[H^+]}\right\}$ $K_1 = 1.75 \times 10^{-5}$ M	9.6×10^5	2
ROOH	$H_{ROOH} = 6$ (lower bound)	No dissociation. Aqueous removal reactions known. Other refs: 227 M atm^{-1} (ref 1)	$H^*_{ROOH} = H_{ROOH}$	> 6	2
ONIT	$H_{ROOH} = 2$	Dissociation unknown	$H^*_{ONIT} = H_{ONIT}$	2	7
INIT	No data available	Assumed similar to ONIT	$H^*_{INIT} = H_{INIT}$	5	
OXBU	No data available	Unknown, Assumed low		Low	
MUCN	No data available	Unknown, Assumed low		Low	

[a] *Sources*: 1: Seinfeld and Pandis (1998); 2: Herrmann et al. (1999); 3: Howard and Meylan (1997); 4: Betterton and Hoffman (1988); 5: Loudon (1984); 6: Gaffney et al. (1987); 7: Sander (1999).

Table 6
pe^0(W) values for various half-redox reactions involving AURAMS species

Species	Reaction	Net change in Gibbs free energy ($J\,mol^{-1}$)	Standard redox potential (V)	pe^0	n_H	pe^0(W)
SO_2	$HSO_3^- + O_2(aq) + H(+) + e^- \rightarrow SO_4(2^-) + H_2O$	−470298	4.874	82.528	1.000	75.53
	$HSO_3^- + O_3(g) + 3\ H(+) + 3e^- \rightarrow SO_4(2^-) + 2\ H_2O$	−854376	2.952	49.975	1.000	42.98
	$SO_3(2^-) + O_2(aq) + 2\ H(+) + 2e^- \rightarrow SO_4(2^-) + H_2O$	−511508	2.651	44.880	1.000	37.88
	$HSO_3^- + O_2\ (aq) + 2\ H(+) + 2e^- \rightarrow HSO_4^- + H_2O$	−481678	2.496	42.263	1.000	35.26
	$SO_3(2^-) + O_3(g) + 4\ H(+) + 4e^- \rightarrow SO_4(2^-) + 2\ H_2O$	−895586	2.320	39.289	1.000	32.29
	$HSO_3^- + O_3\ (g) + 4\ H(+) + 4e^- \rightarrow HSO_4(-) + 2\ H_2O$	−865756	2.243	37.981	1.000	30.98
	$SO_3\ (2^-) + O_3\ (g) + 5\ H(+) + 5e^- \rightarrow HSO_4(-) + 2\ H_2O$	−906966	1.880	31.831	1.000	24.83
	$SO_3\ (2^-) + O_2\ (aq) + 3\ H(+) + 3e^- \rightarrow HSO_4(-) + H_2O$	−481678	1.664	28.175	1.000	21.18
	$4\ SO_2\ (g) + 6e^- + 4\ H(+) \rightarrow S_4O_6\ (2^-) + 2\ H_2O$		**0.511**	**8.652**	**0.666**	**3.99**
	$4\ SO_2(aq) + 6e^- + 4\ H(+) \rightarrow S_4O_6\ (2^-) + 2\ H_2O$	−293724	0.507	8.590	0.666	3.93
	$2\ SO_3\ (2^-) + 4e^- + 6\ H(+) \rightarrow S_2O_3\ (2^-) + 3\ H_2O$		**0.666**	**11.277**	**1.500**	**0.78**
	$2\ HSO_3^- + 4e^- + 4\ H(+) \rightarrow S_2O_3\ (2^-) + 3\ H_2O$		**0.453**	**7.670**	**1.000**	**0.67**
	$SO_2(g) + 4e^- + 4\ H(+) \rightarrow S(s) + 2\ H_2O$		**0.451**	**7.636**	**1.000**	**0.64**
	$SO_2(aq) + 4e^- + 4\ H(+) \rightarrow S(s) + 2\ H_2O$	−173648	0.450	7.618	1.000	0.62
	$4\ SO_3(2^-) + 6e^- + 12\ H(+) \rightarrow S_4O_6\ (2^-) + 6\ H_2O$		**0.862**	**14.595**	**2.000**	**0.60**
	$4\ HSO_3^- + 6e^- + 8\ H(+) \rightarrow S_4O_6\ (2^-) + 6\ H_2O$		**0.577**	**9.770**	**1.333**	**0.44**
	$2\ SO_3\ (2^-) + 2e^- + 4\ H(+) \rightarrow S_2O_4(2^-) + 2\ H_2O4(2^-) + 2\ H_2O$		**0.526**	**8.906**	**2.000**	**−5.09**
	$2\ HSO_3^- + 2e^- + 2\ H(+) \rightarrow S_2O_4(2^-) + 2\ H_2O$		**0.099**	**1.676**	**1.000**	**−5.32**
	$2\ HSO_3^- + 2e^- + 3\ H(+) \rightarrow HS_2O_4^- + 2\ H_2O$		**0.173**	**2.929**	**1.500**	**−7.57**
H_2SO_4	**$3\ H_2SO_3\ (aq) + 2e^- \rightarrow S_3O_6(2^-) + 3\ H_2O$**		**0.290**	**4.910**	**0.000**	**4.91**
	$4\ H_2SO_3\ (aq) + 6e^- + 4\ H(+) \rightarrow S_4O_6\ (2^-) + 6\ H_2O$		**0.507**	**8.584**	**0.666**	**3.92**
	$2\ H_2SO_3\ (aq) + 4e^- + 2\ H(+) \rightarrow S_2O_3\ (2^-) + 3\ H_2O$		**0.400**	**6.773**	**0.500**	**3.27**
	$H_2SO_3\ (aq) + 4e^- + 4\ H(+) \rightarrow S(s) + 3\ H_2O$		**0.500**	**8.466**	**1.000**	**1.47**
	$5\ H_2SO_3\ (aq) + 10e^- + 8H(+) \rightarrow S_5O_6(2^-) + 9\ H_2O$		**0.416**	**7.044**	**0.800**	**1.44**
	$H_2SO_3\ (aq) + 2e^- + 2\ H(+) \rightarrow H_2SO_2 + H_2O$		**0.400**	**6.773**	**1.000**	**−0.23**
	$H_2SO_4(aq) + 6\ H(+) + 6e^- \rightarrow S(s) + 4\ H_2O$	−204082	0.353	5.969	1.000	−1.03
	$H_2SO_4(aq) + 8\ H(+) + 8e^- \rightarrow H_2S(aq) + 4\ H_2O$	−231952	0.300	5.088	1.000	−1.91
	$H_2SO_4(aq) + 2\ H(+) + 2e^- \rightarrow H_2SO_3\ (aq) + H_2O$	−30448	0.158	2.672	1.000	−4.33
	$H_2SO_4(aq) + 2\ H(+) + 2e^- \rightarrow SO_2\ (aq) + 2\ H_2O$	−30434	0.158	2.670	1.000	−4.33
NO	$NO(g) + O_3\ (g) + 3\ H(+) + 3e^- \rightarrow HNO_3(aq) + H_2O$	−598248	2.067	34.994	1.000	27.99
	$NO(g) + O_2\ (aq) + 3\ H(+) + 3e^- \rightarrow HNO_2\ (aq) + H_2O$	−542548	1.874	31.736	1.000	24.74
	$2\ NO(g) + 4\ H(+) + 4e^- \rightarrow N_2(g) + 2\ H_2O$		**1.678**	**28.412**	**1.000**	**21.41**
	$2\ NO(aq) + 2\ H(+) + 2e^- \rightarrow N_2O\ (g) + H_2O$		**1.590**	**26.922**	**1.000**	**19.92**
	$NO(g) + 6\ H(+) + 5e^- \rightarrow NH_4 + + H_2O$		**0.836**	**14.155**	**1.000**	**7.16**
	$NO(g) + 5\ H(+) + 5e^- \rightarrow NH_3 \cdot H_2O(aq)$		**0.727**	**12.310**	**1.000**	**5.31**
	$2\ NO(aq) + 2\ H(+) + 2e^- \rightarrow H_2N_2O_2$		**0.710**	**12.022**	**1.000**	**5.02**
	$2\ NO(aq) + 2e^- \rightarrow N_2O_2\ (2^-)$		**0.180**	**3.048**	**0.000**	**3.05**

NO_2	NO_2 (g) + H(+) + e^- → NO(g) + H_2O	−201908	2.093	35.431	1.000	28.43
	NO_2 (g) + O_3 (g) + 5 H(+) + $5e^-$ → HNO_3 (aq) + 2 H_2O	−800156	1.659	28.082	1.000	21.08
	NO_2 (g) + O_3 (g) + 7 H(+) + $7e^-$ → HNO_2 (aq) + 3 H_2O	−981634	1.453	24.608	1.000	17.61
	NO_2 (g) + O_2 (aq) + 3 H(+) + $3e^-$ → HNO_3 (aq) + H_2O	−416078	1.437	24.338	1.000	17.34
	2 NO_2 (g) + 8 H(+) + $8e^-$ → N_2(g) + 4 H_2O		**1.363**	**23.078**	**1.000**	**16.08**
	NO_2 (g) + e^- → NO_2^-		**0.895**	**15.154**	**0.000**	**15.15**
	NO_2 (g) + O_2 (aq) + 5 H(+) + $5e^-$ → HNO_2 (aq) + 2 H_2O	−597556	1.239	20.972	1.000	13.97
	NO_2 (aq) + 6 H(+) + $6e^-$ → N_2O (g) + 3 H_2O		**1.229**	**20.809**	**1.000**	**13.81**
	NO_2 (g) + H(+) + e^- → HNO_2 (aq)		**1.093**	**18.507**	**1.000**	**11.51**
	NO_2 (g) + 8 H(+) + $8e^-$ → NH_4+ + 2 H_2O		**0.897**	**15.188**	**1.000**	**8.19**
O_3	**O_3(aq) + 2 H(+) + $2e^-$ → O_2 (aq) + H_2O**		**2.075**	**35.134**	**1.000**	**28.13**
	O_3(g) + 2 H(+) + $2e^-$ → O_2 (aq) + H_2O	−384078	1.990	33.699	1.000	26.70
	O_3(g) + 4 H(+) + $4e^-$ → OH(aq) + 2 H_2O	−629816	1.632	27.630	1.000	20.63
	O_3(g) + 6 H(+) + $6e^-$ → 3 H_2O	−874734	1.511	25.583	1.000	18.58
H_2O_2	H_2O_2 (aq) + O_3 (g) + 4 H(+) + $4e^-$ → O_2 (aq) + 3 H_2O	−724334	1.877	31.777	1.000	24.78
	H_2O_2 (aq) + 2 H(+) + $2e^-$ → 2 H_2O		**1.763**	**29.851**	**1.000**	**22.85**
	H_2O_2 (aq) + O_2 (aq) + 6 H(+) + $6e^-$ → 4 H_2O	−830912	1.435	24.301	1.000	17.30
	H_2O_2 (aq) + H(+) + e^- → OH(aq) + H_2O	−95338	0.988	16.730	1.000	9.73
HNO_3	2 HNO_3 (aq) + 10 H(+) + $10e^-$ → N_2(g) + 6 H_2O	−1200468	1.244	21.066	1.000	14.07
	HNO_3 (aq) + O_2 (aq) + 6H(+) + $6e^-$ → HNO_2 (aq) + 3 H_2O	−672134	1.161	19.658	1.000	12.66
	2 HNO_3 (aq) + 8 H(+) + $8e^-$ → N_2O (g) + 5 H_2O	−859090	1.113	18.844	1.000	11.84
	HNO_3 (aq) + 2 H(+) + $2e^-$ → HNO_2 (aq) + H_2O	−181478	0.940	15.923	1.000	8.92
HONO	2 HNO_2 (aq) + 6 H(+) + $6e^-$ → N_2(g) + 4 H_2O	−837512	1.447	24.494	1.000	17.49
	2 HNO_2 (aq) + O_2 (aq) + 10 H(+) + $10e^-$ → N_2(g) + 6 H_2O	−1328168	1.376	23.307	1.000	16.31
	2 HNO_2 (aq) + 4 H(+) + $4e^-$ → N_2O (g) + 3 H_2O	−496134	1.285	21.765	1.000	14.77
HNO_4	HNO_4: expected to be similar to HNO_3, HNO_2 (no ΔG data)					
NH_3	NH_3: won't appear as reactant in reduction reactions					
PAN	*$CH_3C(O)OONO_2$ (g) + H(+) + e^- → 2 HCOOH (aq) + NO(g)*	*−211770*	*2.195*	*37.161*	*1*	*30.16*
	$CH_3C(O)OONO_2$ (g) + 3 H(+) + $4e^-$ → $CH_3C(O)OH$(aq) + N O_2^- + H_2O	*−259918*	*0.673*	*11.403*	*0.75*	*6.15*
	$CH_3C(O)OONO_2$ (g) + H(+) + $2e^-$ → $CH_3C(O)OH$(aq) + NO_3^-	*−97040*	*0.503*	*8.514*	*0.5*	*5.01*
	$CH_3C(O)OONO_2$ (g) + 9 H(+) $10e^-$ → 2 CH_4(g) + NO_3^- + 2 H_2O	*−273384*	*0.283*	*4.797*	*0.9*	*−1.50*
	$CH_3C(O)OONO_2$ (g) + 7 H(+) $8e^-$ → 2 CH_3OH(aq) + NO_2^- + H_2O	*−209318*	*0.271*	*4.591*	*0.875*	*−1.53*
PPN	*$CH_3CH_2C(O)OONO_2$ + H(+) + e^- → $CH_3C(O)OH$(aq) + HCOOH(aq) + NO(g)*	*−255590*	*2.649*	*44.851*	*1.000*	*37.85*
	$CH_3CH_2C(O)OONO_2$ + 3H(+) + $4e^-$ → $CH_3CH_2C(O)OH$(aq) + NO_2^- + H_2O	*−230268*	*0.597*	*10.102*	*0.750*	*4.85*
	$CH_3CH_2C(O)OONO_2$ + 6 H(+) + $7e^-$ → CH_4(g) + $CH_3C(O)OH$(aq) + NO_3^-	*−148254*	*0.219*	*3.717*	*0.857*	*−2.28*

Table 6 (*continued*)

Species	Reaction	Net change in Gibbs free energy ($J\,mol^{-1}$)	Standard redox potential (V)	pe^0	n_H	pe^0(W)
APAN	$C_6H_5C(O)OONO_2 + H(+) + 2e^- \rightarrow C_6H_5C(O)OH + NO_3^-$	*−287010*	*2.975*	*50.365*	*0.500*	*46.86*
	$C_6H_5C(O)OONO_2 + 3H(+) + 4e^- \rightarrow C_6H_5C(O)OH + NO_2^- + H_2O$	*−375888*	*0.974*	*16.490*	*0.75*	*11.24*
MPAN	$H_2CC(CH_3)C(O)OONO_2 + H(+) + 2e^- \rightarrow H_2CC(CH_3)C(O)OH + NO_3^-$	*−75390*	*0.391*	*6.615*	*0.5*	*3.11*
HCHO	**HCHO(aq) + 2e⁻ + 2 H(+) → CH₃OH(aq)**		**0.588**	**9.956**	**1.000**	**2.96**
	$HCHO(aq) + 4e^- + 4\,H(+) \rightarrow CH_4(g) + H_2O$	−158272	0.410	6.943	1.000	−0.06
MCHO	$CH_3CHO(g) + 6\,H(+) + 6e^- \rightarrow 2\,CH_4(g) + H_2O$	−205366	0.355	6.006	1.000	−0.99
	$CH_3CHO(g) + 2\,H(+) + 2e^- \rightarrow C_2H_5OH(aq)$	−35200	0.182	3.088	1.000	−3.91
PALD	$CH_3CH_2CHO(g) + 4\,H(+) + 4e^- \rightarrow C_3H_8(g) + H_2O$	−130168	0.337	5.710	1.000	−1.29
	$CH_3CH_2CHO(g) + 8\,H(+) + 8e^- \rightarrow 3\,CH_4(g) + H_2O$	−259060	0.336	5.682	1.000	−1.32
	$CH_3C(O)CH3(g) + 8\,H(+) + 8e^- \rightarrow 3\,CH_4(g) + H_2O$	−236360	0.306	5.185	1.000	−1.82
C4A	$CH_3CH_2CH_2CHO + 10\,H(+) + 10e^- \rightarrow 4\,CH_4 + H_2O$	−325554	0.337	5.713	1.000	−1.29
	$CH_3CH_2CH_2CH_2CHO + 12\,H(+) + 12e^- \rightarrow 5\,CH_4 + H_2O$	−382748	0.331	5.597	1.000	−1.40
	$CH_3CH_2CH_2C(O)CH_3 + 12\,H(+) + 12e^- \rightarrow 5\,CH_4 + H_2O$	−353948	0.306	5.176	1.000	−1.82
	$CH_3CH_2C(O)CH_3 + 10\,H(+) + 10e^- \rightarrow 4\,CH_4 + H_2O$	−294154	0.305	5.162	1.000	−1.84
C7A	$C_7H_{14}O + 16\,H(+) + 16e^- \rightarrow 7\,CH_4 + H_2O$	*−501276*	*0.325*	*5.498*	*1*	*−1.50*
ACHO	$C_7H_6O(g) + 4\,H(+) + 4e^- \rightarrow C_7H_8(g) + H_2O$	−137478	0.356	6.031	1	−0.97
	$C_7H_6O + 24\,H(+) + 24e^- \rightarrow 7\,CH_4 + H_2O$	−615136	0.266	4.498	1	−2.50
MVK	$CH_3C(O)CHCH_2 + 14\,H(+) + 14e^- \rightarrow 4\,CH_4 + H_2O$	*−498634*	*0.369*	*7.243*	*1*	*0.24*
MACR	$CH_2C(CH_3)CHO + 14\,H(+) + 14e^- \rightarrow 4\,CH_4 + H_2O$	*−402924*	*0.298*	*5.853*	*1*	*−1.15*
MGLY	$CH_3C(O)CHO + 12\,H(+) + 12e^- \rightarrow 3\,CH_4 + 2\,H_2O$	*−372678*	*0.322*	*6.316*	*1*	*−0.68*
MOH	**$CH_3OH(aq) + 2\,H(+) + 2e^- \rightarrow CH_4(g) + H_2O$**		**0.588**	**9.956**	**1.000**	**2.96**
ETOH	$CH_3CH_2OH(aq) + 5\,H(+) + 5e^- \rightarrow 2\,CH_4(g) + H_2O$	−161766	0.335	5.677	1	−1.32
	$CH_3CH_2OH(aq) + 5\,H(+) + 5e^- \rightarrow C_3H_8(g) + H_2O$	−93128	0.241	4.086	1	−2.91
POH	$C_3H_7OH(g) + 6\,H(+) + 6e^- \rightarrow 3\,CH_4 + H_2O$	−227660	0.393	6.658	1	−0.34

CRES	p-C_7H_8O(g) + 22 H(+) + 22e^- → 7 CH_4 + H_2O	−561836	0.265	4.481	1	−2.52
FORM	**HCOOH(aq) + 2 H(+) + 2e^- → C + 2 H_2O**		**0.523**	**8.855**	**1.000**	**1.86**
	HCOOH(aq) + 6 H(+) + 6e^- → CH_4(g) + 2 H_2O	−125550	0.217	3.672	1.000	−3.33
	HCOOH(aq) + 4 H(+) + 4e^- → CH_3OH(aq) + H_2O		**0.100**	**1.693**	**1.000**	**−5.31**
	HCOOH(aq) + 2 H(+) + 2e^- → HCHO(aq) + H_2O		**0.034**	**0.576**	**1.000**	**−6.42**
ACAC	$CH_3C(O)OH$(aq) + 8e^- + 8H(+) → 2 CH_4(g) + 2 H_2O	−176344	0.228	3.868	1.000	−3.13
	$CH_3C(O)OH$(aq) + 4e^- + 4H(+) → C_2H_5OH(aq) + H_2O	−14577.8	0.038	0.640	1.000	−6.36
	$CH_3C(O)OH$(aq) + 4e^- + 4H(+) → 2 CH_3OH(aq)	50600	−0.131	−2.220	1.000	−9.22
	$CH_3C(O)OH$(aq) + 2e^- + 2H(+) → CH_3CHO(aq) + H_2O	29022	−0.150	−2.546	1.000	−9.55
ROOH	*CH_3OOH(aq) + 2 H(+) + 2e^- → CH_3OH(aq) + H_2O*	*−127398*	*0.660*	*11.178*	*1*	*4.18*
	CH_3OOH(aq) + 4 H(+) + 4e^- → CH_4(g) + 2 H_2O	*−240870*	*0.624*	*10.567*	*1*	*3.57*
ONIT	*CH_3ONO_2 + H(+) + e^- → CH_3OH(aq) + NO_2 (−)*	*−99590*	*1.032*	*17.476*	*1.000*	*10.48*
	CH_3ONO_2 + 4 H(+) + 4e^- → CH_4(g) + HNO_2 (aq) + H_2O	*−231662*	*0.600*	*10.163*	*1.000*	*3.16*
	CH_3ONO_2 + 3 H(+) + 3e^- → CH_4(g) + NO_2 (g) + H_2O	*−124762*	*0.431*	*7.298*	*1.000*	*0.30*
	CH_3ONO_2 + H(+) + e^- → CH_3OH(aq) + NO_2 (g)	*−11290*	*0.117*	*1.981*	*1.000*	*−5.02*
CO	CO + 2 H(+) + 2e^- → C(s) + H_2O		0.517	8.754	1.000	1.75
OXBU	*CH(O)CHCHCHO + 16 H(+) + 16e^- → 4 CH_4 + 2 H_2O*	*−552552*	*0.358*	*7.023*	*1*	*0.02*
MUCN	*$CH_3C(O)CHCHCHCHCHO$ + 24 H(+) + 24e^- → 7 CH_4 + 2 H_2O*	*−792054*	*0.342*	*6.712*	*1*	*−0.29*
OH	2 OH(g) + 4 H(+) + 4e^- → H_2(g) + 2 H_2O	−542796	1.406	23.813	1	16.81
HO_2	2 HO_2 (aq) + 8 H(+) + 8e^- → H_2(g) + 4 H_2O	−957592	1.241	21.004	1	14.00
MO_2	CH_3O_2 (g) + H(+) + e^- → C(s) + 2 H_2O	−274276	2.843	48.130	1	41.13

may be related to the change in Gibbs free energy for the reaction (ΔG) or to the standard redox potential (E_H^0):

$$pe^0 = \frac{F\,E_H^0}{2.3\,RT} = -\frac{\Delta G}{2.3nRT},$$

where F is Faraday's constant (9.6489×10^4 C/mol) and $R = 8.314\,\mathrm{J\,mol^{-1}\,K^{-1}}$. In addition to measured values of ΔG and E_H^0, estimates of ΔG may be obtained through calculating the change in Gibbs free energies of formation for the components of the reactions.

In Table 6, ΔG, E_H^0, pe^0, n_H, and $pe^0(W)$ are shown for a number of half-redox reactions relating to gas-phase species considered in the manuscript. Boldface entries indicate values determined from experiments tabulated in Bard et al. (1985). Regular type indicates values calculated from ΔG or E_H^0 values tabulated in Bard et al. (1985) or Reid et al. (1987). Italicized type indicates estimates from ΔG's calculated using group methods (Joback Method, as outlined in Reid et al. (1987)). Note that ΔG values are not given when experimentally determined E_H^0 values are available. Also, 12 AURAMS unoxygenated VOC classes have not been included in Table 6 since they will not participate in aqueous-phase redox reactions.

References

Andersen, H.V., Hovmand, M.F., 1995. Ammonia and nitric acid dry deposition and throughfall. Water, Air and Soil Pollution 85, 2211–2216.

Andersen, H.V., Hovmand, M.F., Hummelshoj, P., Jensen, N.O., 1999. Measurement of ammonia concentration, flux and dry deposition velocities to a spruce forest 1991–1995. Atmospheric Environment 33, 1367–1383.

Baldocchi, D., Meyers, T., 1998. On using eco-physiological, micrometeorological and biogeochemical theory to evaluate carbon dioxide, water vapor and trace gas fluxes over vegetation: a perspective. Agricultural and Forest Meteorology 90, 1–25.

Bard, A.J., Parsons, R., Jordan, J., 1985. Standard Potentials in Aqueous Solution. M. Dekker, New York, 834 pp.

Betterton, E.A., Hoffman, M.R., 1988. Henry's Law constants of some environmentally important aldehydes. Environmental Science and Technology 22, 1415–1418.

Bottger, A., Ehhalt, D.H., Gravenhorst, G., 1980. Atmospharische Kreislaufe von Stickstoffoxiden and Ammoniak, Tept. Jul-15582. Auflage (1980), Kernforschungsanlage Julich. BRD.

Brook, J., Zhang, L., Digiovanni, F., Padro, J., 1999. Description and evaluation of a model for routine estimates of air pollutant dry deposition over North America. Part I: Model devlopment. Atmospheric Environment 33, 5037–5051.

Chamel, A., Gambonnet, B., 1997. Sorption and diffusion of an ethoxylated stearic alcohol and ethoxylated stearic amine into and through isolated plant cuticles. Chemosphere 34, 1777–1786.

Dabney, S.M., Bouldin, D.R., 1990. Apparent deposition velocity and compensation point of ammonia inferred from gradient measurements above and through Alfalfa. Atmospheric Environment 24, 2655–2666.

Dickinson, R.E., Henderson-Sellers, A., Kennedy, P.J., Wilson, M.F., 1986. Biosphere—atmosphere transfer scheme (BATS) for the NCAR community climate model. NCAR Technical Note NCAR/TN275 + STR, National Center for Atmospheric Research, Boulder, CO, 67 pp.

Dollard, G.J., Atkins, D.H.F., Davies, T.J., Healy, C., 1987. Concentrations and dry deposition velocities of nitric acid. Nature 326, 481–483.

Dollard, G.J., Jones, B.M.R., Davies, T.J., 1990. Dry deposition of HNO_3 and PAN. Atomic Energy Research Establishment. Report R13780, Atomic Energy Research Establishment, Harwell, Oxfordshire.

Dorman, J.L., Sellers, P.J., 1989. A global climatology of albedo, roughness length and stomatal resistance for atmospheric general circulation models as represented by the simple biosphere model (SiB). Journal of Applied Meteorology 28, 833–855.

Duyzer, J.H., Verhagen, H.L.M., Weststrate, J.H., Bosveld, F.C., 1992. Measurement of the dry deposition of NH_3 onto coniferous forest. Environmental Pollution 75, 3–13.

Duyzer, J.H., Verhagen, H.L.M., Weststrate, J.H., Bosveld, F.C., 1994. The dry deposition of ammonia onto a Douglas fir forest in the Netherlands. Atmospheric Environment 28, 1241–1253.

Erisman, J.W., Wyers, G.P., 1993. Continuous measurements of the surface exchange of SO_2 and NH_3: implications for their possible interaction in the deposition process. Atmospheric Environment 27A, 1937–1949.

Erisman, J.W., van Elzakker, B.G., Mennen, M.G., Hogenkamp, J., Zwart, E., van den Beld, L., Römer, F.G., Bobbink, R., Heil, G., Raessen, M., Duyzer, J.H., Verhage, H., Wyers, G.P., Otjes, R.P., Mols, J.J., 1994a. The Elspeetsche Veld experiment on surface exchange of trace gases: summary of results. Atmospheric Environment 28, 487–496.

Erisman, J.W., Van Pul, A., Wyers, P., 1994b. Parameterization of surface resistance for the quantification of atmospheric deposition of acidifying pollutants and ozone. Atmospheric Environment 28, 2595–2607.

Eugster, W., Hesterberg, R., 1996. Transfer resistances of NO_2 determined from eddy correlation flux measurements over a little meadow at a rural site on the Swiss plateau. Atmospheric Environment 30, 1247–1254.

Finkelstein, P.L., Ellestad, T.G., Clarke, J.F., Meyers, T.P., Schwede, D., Hebert, E.O., Neal, J.F., 2000. Ozone and sulfur dioxide dry deposition to forests: observations and model evaluation. Journal of Geophysical Research 105, 15365–15377.

Flechard, C.R., Fowler, D., Sutton, M.A., Cape, J.N., 1999. A dynamic chemical model of bi-directional ammonia exchange between semi-natural vegetation and the atmosphere. Quarterly Journal of the Royal Meteorological Society 125, 2611–2641.

Gaffney, J.S., Streit, G.E., Spall, W.D., Hall, J.H., 1987. Beyond acid rain: do soluble oxidants and organic toxins interact with SO_2 and NO_x to increase ecosystem effects. Environmental Science and Technology 21, 519–524.

Garland, J.A., Penkett, S.A., 1976. Absorption of peroxy acetyl nitrate and ozone by natural surfaces. Atmospheric Environment 10, 1127–1131.

Gong, S.L., Barrie, L.A., Blanchet, J.-P., von Salzen, K., Lohmann, U., Lesins, G., Spacek, L., Zhang, L., Girard, E., Lin, H., Leaitch, R., Leighton, H., Chylek, P., Hung, P., Jiang, J., 2001. CAM: a size segregated simulation of atmospheric aerosol processes for climate and air quality models. Part 1. Module development. Journal of Geophysical Research, submitted for publication.

Gravenhorst, G., Bottger, A., 1982. Field measurements of NO and NO_2 fluxes to and from the ground. In: Beilke, S., Elshout, A.J. (Eds.), Acid Deposition. Reidel, Dordrecht, pp. 172–184.

Hall, B., Claiborn, C., 1997. Measurement of the dry deposition of peroxides to a Canadian boreal forest. Journal of Geophysical Research 102, 29343–29353.

Hall, B., Claiborn, C., Baldocchi, D., 1999. Measurement and modelling of the dry deposition of peroxides. Atmospheric Environment 33, 577–589.

Harrison, R.M., Kitto, A.N., 1994. Evidence for a surface source of atmospheric nitrous acid. Atmospheric Environment 28, 1089–1094.

Harrison, R.M., Rapsomanikis, S., Turnbull, A., 1989. Land–surface exchange in a chemically reactive system: surface fluxes of HNO_3, HCl and NH_3. Atmospheric Environment 23, 1795–1800.

Hartmann, W.R., Santana, M., Hermoso, M., Andreae, M.O., Sanhueza, E., 1991. Diurnal cycles of formic and acetic acids in the northern part of the Guayana Shield. Journal of Atmospheric Chemistry 13, 63–72.

Herrmann, H., Evrens, B., Nowacki, P., Wolke, R., Zellner, R., 1999. A chemical aqueous phase radical mechanism for tropospheric chemistry. Chemosphere 38, 1223–1232.

Hill, A.C., 1971. Vegetation: a sink for air pollutants. Journal of Air Pollution Control Association 21, 341–346.

Howard, P.H., Meylan, W.M., 1997. Handbook of Physical Properties of Organic Chemicals. CRC Lewis Publishers, Boca Raton, 1585 pp.

Huebert, B.J., Robert, C.H., 1985. The dry deposition of nitric acid to grass. Journal of Geophysical Research 90, 2085–2090.

Loudon, G.M., 1984. Organic Chemistry. Addison-Wesely Publishing Co., Reading, MA, 1451 pp.

Massman, W.J., 1999. A model study of κB_H^{-1} for vegetated surfaces using 'localized near-field' Lagrangian theory. Journal of Hydrology 223, 27–43.

Massman, W.J., Pederson, J., Delany, A., Grantz, D., den Hartog, G., Neumann, H.H., Oncley, S.P., Pearson, R., Shaw, R.H., 1994. An evaluation of the regional acid deposition model surface module for ozone uptake at three sites in the San Joaquin Valley of California. Journal of Geophysical Research 99, 8281–8294.

Meeson, B.W., Corprew, F.E., McManus, J.M.P., Myers, D.M., Closs, J.W., Sun, K.-J., Sunday, D.J., Sellers, P.J., 1995. TSLSCP Initiative I—Global data sets for land-atmosphere models, 1987–1988. Vol. 1–5. Published on CD by NASA (USA_NASA_GDAAC_ISLSCP_001-USA_NASA_GDAAC_ISLSCP_005).

Meyers, T.P., Finkelstein, P.L., Clarke, J., Ellestad, T.G., Sims, P.F., 1998. A multi-layer model for inferring dry deposition using standard meteorological measurements. Journal of Geophysical Research 103 (D17), 22645–22661.

Moran, M.D., Scholtz, M.T., Slama, C.F., Dorkalam, A., Taylor, A., Ting, N.S., Davies, D., Makar, P.A., Venkatesh, S., 1997. An overview of CEPS1.0: Version 1.0 of the Canadian emissions processing system for regional-scale air quality models. Proceedings of the Seventh AWMA Emission Inventory Symposium, October 28–30, Research Triangle Park, North Carolina, Air and Waste Management Association, Pittsburgh.

Moran, M.D., Dastoor, A., Gong, S.L., Gong, W., Makar, P.A., 1998. Proposed conceptual design for the AES regional particulate matter model/unified model. Unpublished Report, Meteorological Service of Canada, Downsview, Ont., Canada, 100 pp [Available from first author].

Norman, J.M., 1982. Simulation of microclimates. In: Hatfield, J.L., Thompson, I.J. (Eds.), Biometeorology in Integrated Pest Management. Academic Press, New York, pp. 65–99.

Padro, J., 1996. Summary of ozone dry deposition velocity measurements and model estimates over vineyard, cotton, grass and deciduous forest in summer. Atmospheric Environment 30, 2363–2369.

Padro, J., den Hartog, G., Neumann, H.H., 1991. An investigation of the ADOM dry deposition module using summertime O_3 measurements above a deciduous forest. Atmospheric Environment 25, 1689–1704.

Padro, J., Neumann, H.H., den Hartog, G., 1992. Modelled and observed dry deposition velocity of O_3 above a deciduous forest in the winter. Atmospheric Environment 26, 775–784.

Padro, J., Zhang, L., Massman, W.J., 1998. An analysis of measurements and modelling of air–surface exchange of NO–NO_2–O_3 over grass. Atmospheric Environment 32, 1365–1375.

Pilegaard, K., Hummelshøj, P., Jensen, N.O., 1998. Fluxes of ozone and nitrogen dioxide measured by eddy correlation over a harvested wheat field. Atmospheric Environment 32, 1167–1177.

Pleim, J., Venkatram, A., Yamartino, R., 1984. ADOM/TADAP Model Development Program. The Dry Deposition Module, Vol. 4. ERT Document No. PB980-520, Environmental Research and Technology, Inc., Concord, MA.

Pudykiewicz, J.A., Kallaur, A., Smolarkiewicz, P.K., 1997. Semi-Lagrangian modelling of tropospheric ozone. Tellus 49B, 231–248.

Reid, R.C., Prausnitz, J.M., Poling, B.E., 1987. The Properties of Gases and Liquids, 4th Edition. McGraw-Hill, Inc., New York, 741 pp.

Rondón, A., Johansson, C., Granat, L., 1993. Dry deposition of nitrogen dioxide and ozone to coniferous forests. Journal of Geophysical Research 98, 5159–5172.

Sander, R., 1999. Compilation of Henry's Law constants for inorganic and organic species of potential importance in environmental chemistry (version 3). http://www.mpch-mainz.mpg.de/~sander/res/henry.html.

Sanhueza, E., Santana, M., Hermoso, M., 1992. Gas and aqueous-phase formic and acetic acids at a tropical cloud forest site. Atmospheric Environment 26, 1421–1426.

Seinfeld, J., Pandis, S., 1998. Atmospheric Chemistry and Physics. Wiley, New York, 1326pp.

Sellers, P.J., Randall, D.A., Collatz, J.G., Berry, J.A., Field, C.B., Dazlich, D.A., Collelo, G.D., Bounoua, L., 1996. A revised land surface parameterization (SiB2) for atmospheric GCMS Part I: model formulation. Journal of Climate 9, 676–705.

Smith, R.I., Fowler, D., Sutton, M.A., Flechard, C., Coyle, M., 2000. Regional estimation of pollutant gas dry deposition in the UK: model description, sensitivity analyses and outputs. Atmospheric Environment 34, 3757–3777.

Stumm, W., Morgan, J.J., 1996. Aquatic Chemistry: Chemical Equilibria and Rates in Natural Waters. Wiley, New York, 1003 pp.

Sutton, M.A., Moncrieff, J.B., Fowler, D., 1992. Deposition of atmospheric ammonia to moorlands. Environmental Pollution 75, 15–24.

Sutton, M.A., Burkhardt, J.K., Guérin, D., Nemitz, E., Fowler, D., 1998. Development of resistance models to describe measurements of bi-directional ammonia surface–atmosphere exchange. Atmospheric Environment 32, 473–480.

Venkatram, A., Karamchandani, P.K., Misra, P.K., 1988. Testing a comprehensive acid deposition model. Atmospheric Environment 22, 737–747.

Wahner, A., Krinke, S., 2000. Formaldehyde and ozone deposition velocities determined above a deciduous forest during summer. Sixth International Conference on Air–Surface Exchange of Gases and Particles, 3–7 July, Edinburgh, UK. Abstract only.

Walton, S., Gallagher, M.W., Choulanton, T.W., Duyzer, J., 1997. Ozone and NO_2 exchange to fruit orchards. Atmospheric Environment 31, 2767–2776.

Weiss, A., Norman, J.M., 1985. Partitioning solar radiation into direct and diffuse visible and near infrared components. Agricultural and Forest Meteorology 34, 205–214.

Wesely, M.L., 1989. Parameterization of surface resistances to gaseous dry deposition in regional-scale numerical models. Atmospheric Environment 23, 1293–1304.

Wesely, M.L., Hicks, B.B., 2000. A review of the current status of knowledge in dry deposition. Atmospheric Environment 34, 2261–2282.

Wesely, M.L., Cook, D.R, Williams, R.M., 1981. Field measurements of small ozone fluxes to snow, wet bare soil and lake water. Boundary Layer Meteorology 20, 459–471.

Wyers, G.P., Erisman, J.W., 1998. Ammonia exchange over coniferous forest. Atmospheric Environment 32, 441–451.

Yienger, J.J., Levy II, H., 1995. Empirical model of global soil-biogenic NO_x emissions. Journal of Geophysical Research 100, 11447–11464.

Zhang, L., Brook, J., Vet, R., Shaw, M., Finkelstein, P., 2001a. Evaluation and improvement of a dry deposition model using SO_2 and O_3 measurements over a mixed forest. Water, Air and Soil Pollution, in press.

Zhang, L., Gong, S., Padro, J., Barrie, L., 2001b. A size-segregated particle dry deposition scheme for an atmospheric aerosol module. Atmospheric Environment 35, 549–560.

Zhang, L., Moran, M.D., Brook, J.R., 2001c. A comparison of models to estimate in-canopy photosynthetically active radiation and their influence on canopy stomatal resistance. Atmospheric Environment 35, 4463–4470.